AD_____

Award Number: W81XH-06-1-0621

TITLE: Development of a Biosensor for Identifying Novel Endocrine-Disrupting Chemicals

PRINCIPAL INVESTIGATOR: Laurel J. Standley, Ph.D.

CONTRACTING ORGANIZATION: Silent Spring Institute
Newton, MA 02458

REPORT DATE: February 2008

TYPE OF REPORT: Final

PREPARED FOR: U.S. Army Medical Research and Materiel Command
Fort Detrick, Maryland 21702-5012

REPORT DOCUMENTATION PAGE

Form Approved
OMB No. 0704-0188

1. REPORT DATE	2. REPORT TYPE	3. DATES COVERED
17-02-2008	Final	18 JUL 2006 - 17 JAN 2008

4. TITLE AND SUBTITLE
Development of a Biosensor for Identifying Novel Endocrine-Disrupting Chemicals

5a. CONTRACT NUMBER

5b. GRANT NUMBER
W81XH-06-1-0621

5c. PROGRAM ELEMENT NUMBER

6. AUTHOR(S)
Laurel J. Standley, Ph.D.

Email: standley@silentspring.org

5d. PROJECT NUMBER

5e. TASK NUMBER

5f. WORK UNIT NUMBER

7. PERFORMING ORGANIZATION NAME(S) AND ADDRESS(ES)

Silent Spring Institute
Newton, MA 02458

8. PERFORMING ORGANIZATION REPORT NUMBER

9. SPONSORING / MONITORING AGENCY NAME(S) AND ADDRESS(ES)
U.S. Army Medical Research and Materiel Command
Fort Detrick, Maryland 21702-5012

10. SPONSOR/MONITOR'S ACRONYM(S)

11. SPONSOR/MONITOR'S REPORT NUMBER(S)

12. DISTRIBUTION / AVAILABILITY STATEMENT
Approved for Public Release; Distribution Unlimited

13. SUPPLEMENTARY NOTES

14. ABSTRACT

Substantial evidence indicates that endocrine disrupting chemicals (EDCs) – particularly those that interact with the estrogen receptor – may play a role in reproduction and hormonal cancers in humans and animals. EDCs can mimic or alter the action of the endogenous hormones, which have been shown to affect the reproductive and endocrine systems of mammals and reptiles. EDCs are found in food, water, air, and consumer products and originate from pharmaceutical, industrial, agricultural, and natural sources. Most chemicals in commerce, and their environmental degradation products, have not been screened to identify EDCs. We have investigated a novel technology – an estrogen-receptor quartz crystal microbalance (ER-QCM) biosensor – to break through this barrier in identifying EDCs. The ER-QCM detects estrogenic substances using a genetically engineered construct of the hormone-binding domain of the estrogen receptor immobilized to a piezoelectric quartz crystal. The ER-QCM detects the presence of ligands that are known to bind the ER and shows no response for non-binding substances such as testosterone and progesterone. Our ultimate goal is to develop the ER-QCM biosensor as a robust tool for identifying estrogenic activity in complex environmental mixtures and to combine the biosensor with other biophysical methods in order to identify novel estrogenic chemicals in a number of environmental matrices. Experiments were done to determine the viability of ER-QCM for this novel purpose.

15. SUBJECT TERMS
None listed.

16. SECURITY CLASSIFICATION OF:			17. LIMITATION OF ABSTRACT	18. NUMBER OF PAGES	19a. NAME OF RESPONSIBLE PERSON
a. REPORT	b. ABSTRACT	c. THIS PAGE			USAMRMC
U	U	U	UU	50	19b. TELEPHONE NUMBER *(include area code)*

Table of Contents

Page

Introduction…….……..….. 2

Body…….. 2

Key Research Accomplishments…….…….. 16

Reportable Outcomes…… 17

Conclusion…… 18

References……. 18

Appendices…… 21

Introduction

Estrogens such as 17-β-estradiol and estrone are steroid compounds that are key mediators of female reproductive functions. In addition, these compounds are essential for health of numerous tissues such as maintenance of bone tissue and are implicated in the cardiovascular system. It has been shown that exogenous chemicals with estrogenic and/or anti-estrogenic activities may disrupt these regulatory pathways.(*1*) Environmental or industrial compounds and phytoestrogens that interfere with the hormonal or endocrine system have been defined as endocrine disrupting chemicals (EDCs). It is well established that these substances cause adverse effects on human health including reproductive cancers by dramatically altering the pattern of gene expression. (*2*)The estrogen receptor is the primary target for these substances because this receptor is promiscuous in its ability to interact with a variety of ligands.(*3, 4*) EDCs mimic estrogen in their ability to induce or inhibit estrogenic responses after binding to the estrogen receptor.

Predicting the estrogenicity of the thousands of compounds present in commerce by structural analysis is difficult since a wide variety of potentially estrogenic substances may bear no resemblance to that of the natural estrogens. Monitoring and detection strategies cannot be grounded on simple analysis of complex environmental samples for known or suspected structures. Many of these compounds or their metabolites may be constituents of food, household or personal care products, or pharmaceuticals.

In this project, a structurally independent ligand-binding domain of the estrogen receptor (HBD) will be produced using genetic engineering.(*5*) The goals of this project are to attach a self assembled layer of this HBD on the surface of a piezoelectric quartz microbalance to produce a biosensor capable of screening environmental samples for small molecules that have estrogenic and antiestrogenic activity. The strategy presented here was designed to allow a screening mechanism and capture system for substances that bind to the estrogen receptor. The development of such a system would impact the risk assessment of a number of compounds including phytoestrogens and other synthetic chemicals, which may potentially modulate endocrine responses leading to greater incidence rates of hormonally-related diseases such as breast cancer.

Body

Instrumentation used in this study

Biosensors are analytical devices that measure the presence of molecular species by combining the intimate recognition properties of biological macromolecules with a signal transduction mechanism. (*6*) An affinity sensor can be designed to detect substances that bind to a particular protein and can be highly specific for that event. Since we are interested in sensing compounds that bind to the estrogen receptor, our sensor incorporates the hormone-binding domain of the estrogen receptor (HBD) as the biomolecule on the surface of this sensor. A signal will be detected from the biosensor when a molecule interacts with HBD. The sensitivity of the biosensor is due to the fact that the HBD only binds certain substances. The HBD is known to be functionally independent as a truncated receptor (amino acids 304-554). When a ligand binds, the protein undergoes a conformational change, which *in vivo* allows interaction with a

variety of factors to propagate the gene action.(*7*) It has been confirmed by X-ray analysis that the conformation of the receptor is solely dependent on the structure of the ligand in the binding pocket.(*8-11*) In the estrogen-occupied receptor, the infamous helix-12 caps the binding pocket and the protein forms a stable complex. Anti-estrogenic substances such as tamoxifen result in a structure where helix-12 is misaligned with the binding pocket.(*8, 12*) We take advantage of this conformational change and change in protein rigidity to detect the binding event by a piezoelectric transducer, namely the QCM. For our studies we used two different QCMs, the Maktec model (Figure 1.) and the Q-Sense Model (Figure 3).

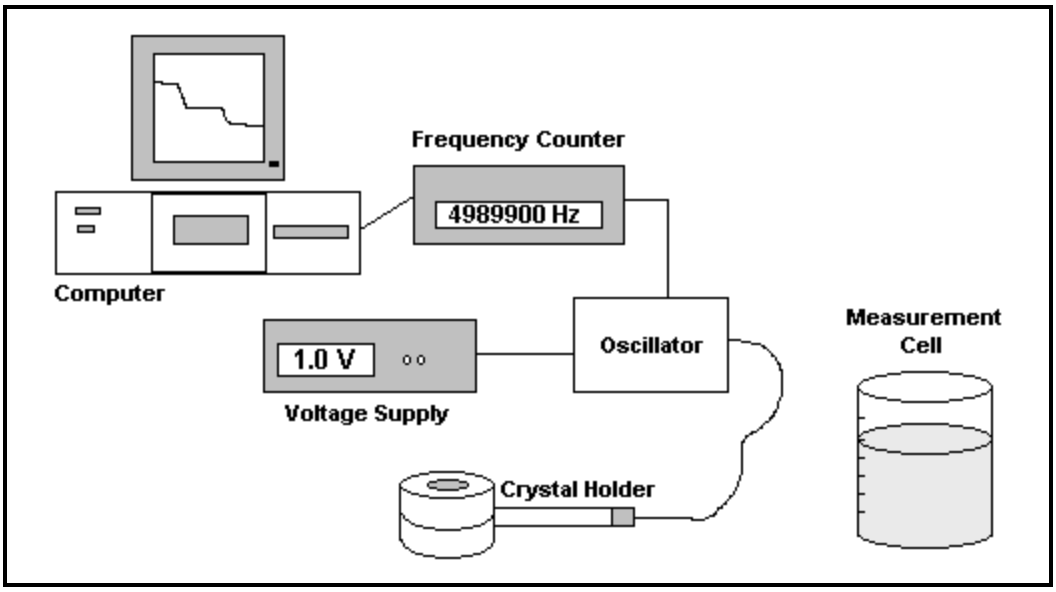

Figure 1. Quartz crystal microbalance measurement system. The crystal holder contains the piezoelectric crystal coated with gold. The crystal has a frequency that is related to the buffer in the measurement cell and the substances attached to the gold surface. Frequency measurements are taken by immersing the crystal holder into the measurement cell and waiting until a steady baseline is obtained. The initial baseline is taken and then protein is added to the crystal and incubated for a period of time. After the incubation the measurement is taken. The ligand is then added to the crystal, which is also incubated for a specific time before the measurement is taken. Crystal frequency usually decreases as mass is added.

Figure 2. Glass cell for the Maxtec instrument. The glass container holds up to 30 ml of liquid. The quartz crystal is located in the area of the clamp. Liquids can be injected into the cell via the rubber stopper at the top of the glass container. For some of our experiments we inserted a small spin bar to mix solutions. Illustration taken from www.infitron.com who has just bought out Maxtec, INC.

Figure 3. The E4 Q-Sense instrument. (The Q-sense instrument used for this study was located in the laboratory of Nathalie Tufenkji Assistant Professor Department of Chemical Engineering McGill University, Canada. Illustration downloaded from Q_sense.com.)

The Q-sense instrument is a state of the art instrument that has a new way of measuring the crystal frequency called the QCM-D technology. The QCM-D monitors the response of a freely oscillating crystal which is touted to be more accurate than other models such as the Maxtec. The QCM-D also measures many different frequencies (called overtones) and dissipation, which is their proprietary technology. The advantage of this technology is the characterization of protein surfaces on the crystal. It was thought that with the dissipation measurement it is possible to determine whether the absorbed film is rigid or soft. Another advantage is the ability to monitor four cells at one time in a flow cell arrangement. Flow cell technology would be a more versatile set up for work in the environment. In addition, our original hypothesis was that the estrogen receptor became more rigid when ligands were bound in the pocket.(*13, 14*) Experiments were run on this instrument in hopes that we could prove that hypothesis and discriminate between different types of ligands. It was also thought that this instrument would be more sensitive than our Maxtec instrument. The crystals have a different design and are

smaller. These gold crystals are cleaned using a pirrhana solution, which strips the entire crystal of all impurities. The surface is smoother than that of the Maxtec crystals.(*13*)

Proteins used in this study

The estrogen receptor is a 66 kDa protein with a number of functional domains. It is fortunate that the hormone HBD can function independently from the intact protein and binds hormone in the same range as the full receptor (*15-17*). Our preliminary studies have used HBD made from a construct that produces the protein from amino acid 304 to 554 (*18-20*). There are four naturally occurring cysteine residues present in this HBD protein: 381, 417, 447 and 530. In order to attach the protein to the gold in a known orientation, it was necessary to have only one cysteine accessible for binding to the gold surface. The cysteine at position 447 is deeply buried within a hydrophobic region of the folded protein and thus is not able to react with the gold film. Since cysteines 381, 417 and 530 are surface exposed, two of these residues (C381 and C530) were mutated to serines, removing their reactivity with the gold surface. From previous work in the Katzenellenbogen laboratory, these mutations are known to have no implications on the overall three dimensional structure of the protein or its capacity to bind ligands (*19, 21*). The one remaining surface exposed cysteine, 417, was then utilized to immobilize the protein on the gold surface. Amino acid 417 is not involved in ligand binding and tethers the protein to the surface in a manner that does not disrupt ligand binding, dimer formation or any conformational change associated with the binding site. Immobilization of the double serine mutant HBD (HBDC417) dimer to the gold electrode is shown in Figure 4.

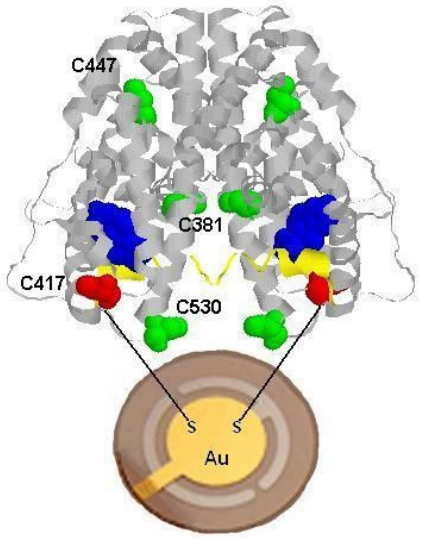

Figure 4. The depiction of the HBDC417 dimer on the gold surface. The cysteine residues in green are labeled. The surface exposed cysteine 417 is illustrated in red and the 17β-estradiol (E_2) is shown in blue. Mutation of Cys to Ser were made on residues

530 and 381. Residue C447 is buried and is not available for binding on the gold surface unless the protein is unfolded. Helix 12 the cap of the binding pocket is shown in yellow.

The HBDC417 immobilized on the surface constitutes the bio part of the biosensor. The frequency of the sensor crystal was measured before and after immobilization of the HBD mutant as well as following exposure to a number of different potential ligands. Repeat experiments with HBDC417 mutant showed frequency shifts resulting from receptor immobilization ranged from 45 - 54 Hz. Exposure of immobilized receptor to 17β-estradiol (natural estrogen) showed an additional frequency shift of 25 Hz. Calculations based only on mass (equation 1) indicate that a frequency shift of less than 1 Hz is expected from addition of 17β-estradiol to the surface. Again, ***an unexpectedly large frequency shift is observed with ligand binding.*** This occurs because of conformational changes in the receptor that change the nanoscale environment at the sensor surface, yielding a much larger frequency response than expected from mass considerations alone. This data was found with the Maxtec system and was reported. (*14*) Our studies funded by this grant further investigate the versatility of the Maxtec system for binding a number of different ligands under the same conditions as reported and to test the sensitivity of the system to ligand concentrations and conditions that would exist in environmental samples.

Another mutant of the HBD was produced for this investigation in hopes that this new construct may provide greater sensitivity, producing a signal in the low nM range for estradiol and other target compounds such as nonylphenol. Sensitivity to a range of estrogens at environmentally-relevant concentrations is a prerequisite to a biosensor and capture system that can be used to monitor unprocessed, relatively uncontaminated field samples. A new HBD construct was made in which we leave the naturally-occurring cysteine at the 530 residue to make the sulfur linkage to the gold surface and mutate the cysteine at position 417 to serine. The illustration of this construct HBDC530 is shown in Figure 5.

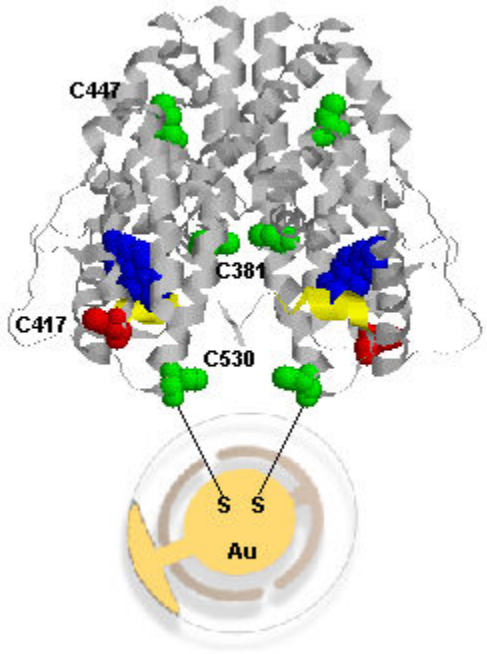

Figure 5. The depiction of the HBDC530 dimer on the gold surface. The surface exposed cysteine 530 is illustrated in green with lines drawn to the gold and the 17β-Estradiol is shown in blue. Mutation of Cys to Ser were made on residues 417 and 381. Residue C447 is buried and is not available for binding on the gold surface unless the protein is unfolded. Helix 12 the cap of the binding pocket is shown in yellow.

A third mutant was also developed for these studies. The triple mutant where all three cysteines were mutated to serine (HBD TM) was produced to provide a negative control for these experiments. If a cysteine is not surface available the immobilization of the protein is not possible and the biosensor will have no change in frequency when protein is added. This provides a check for our hypothesis that the cysteines are key to the immobilization of the protein. In addition this, HBD TM provides a means of ligand capture. If the gold surface of the crystal with HBDC417 immobilized on the surface is fully loaded with ligand a mobile protein HBD TM could be introduced in the experiment. HBD TM in higher concentration than HBDC417 would confiscate the bound ligand by LeChatelier's principal. The mobile protein could then be used for mass spectral studies. We were in hopes that this may be a way to sequester the ligands immobilized on the surface without hindering the protein layer. Severe chemical conditions must be utilized to remove the protein covalently bound on the surface. The conditions make it impossible for the protein to remain intact. If we were to use harsh conditions the proteins would also be compromised. In essence we would have numerous chemical species in a mixture if we were to try to remove the protein (with acid or base conditions) with ligand attached. It would be impossible to sort out the products in a mass spectrometry experiment. So our reasoning for this mutant is to develop a capture and recapture system for future mass spectrometry experiments to discover novel ligands of the estrogen receptor.

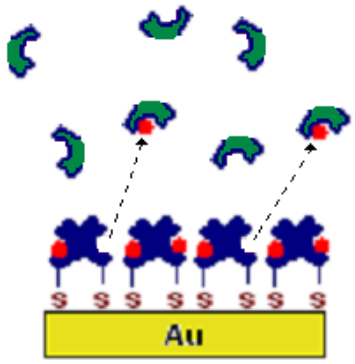

Figure 6. The experimental plan for regeneration of the biosensor surface and sequestering of the ligands captured. Our reasoning for the production of the HBD TM shown in green is to capture the ligands that are sequestered from the environmental samples by the protein immobilized on the surface. We intend to do this so that we would not have to use acid or base to break the covalent S-Au bond. The acid or base would have dire consequences on the protein and make an impossibly complex mixture to examine by mass spectrometry.

Mass spectrometry experiments are being done by Owen Nadeau at University of Kansas Medical Center on the HBD TM. All attempts were made on an FT ICR MS. The proteins were injected onto RP nanobore C18 columns and analyzed by electrospray ionization (ESI). We tried to mimic the procedures outlined in a previously reported work.(20) except that we used fourier transformation for detection. Progress is being made to solubilize the protein so that this methodology can be used.

Both mutants were produced and purified to homogeneity. A representative SDS gel is shown below in Figure 7.

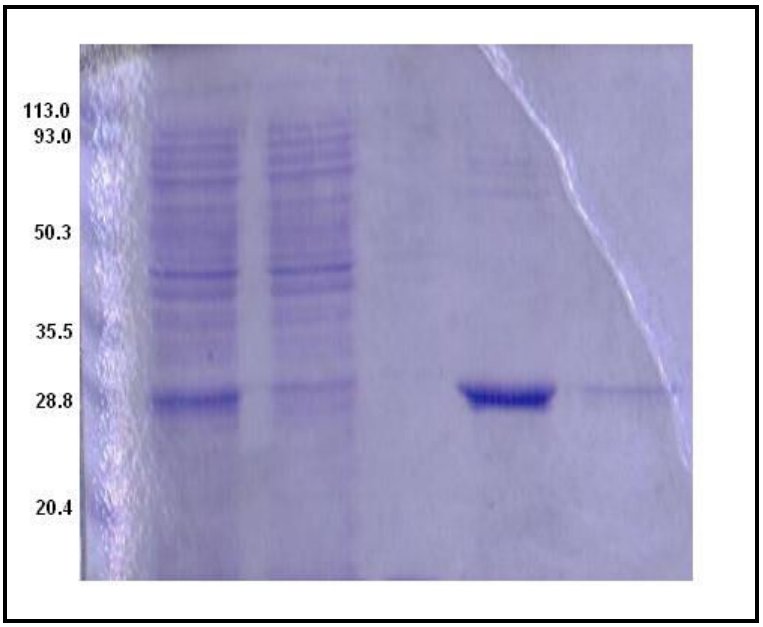

Figure 7 SDS-PAGE of HBD-Mutant expression and isolation: Lane 1- molecular weight marker; Lane 2- supernatant from lysed cells; Lane 3- supernatant run-thru from Ni(II)-NTA column; Lane 4- T/G buffer run-thru column; Lane 5- HBD-Mutant elution #1 from column; Lane 6- HBD-Mutant elution #2 from column. Details of the purification are published. (*14, 22*)

The following is a graph of the experiments with HBDC417 and a number of ligands. The ligand concentration for each of these is 20 uM with less than 10% ethanol in solution.(*14*)

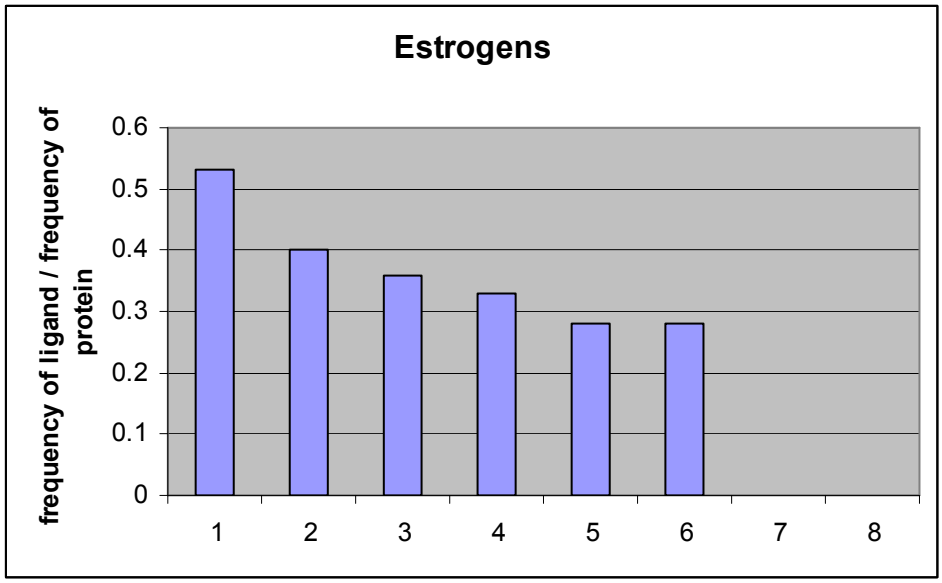

Figure 8. QCM Frequency Response to Ligand Binding. This graph represents the frequency shifts from the QCM for ligand binding relative to the immobilization of HBD-C417 for two trials with each ligand. Ligand include: (1) 17B-estradiol (2) estriol (3)

diethylstilbestrol (4) tamoxifen (5) 4-hydroxytamoxifen (6) genistein (7) testosterone and (8) progesterone. Experiments were done with 20 μM ligand with less than 10% ethanol in the buffer.

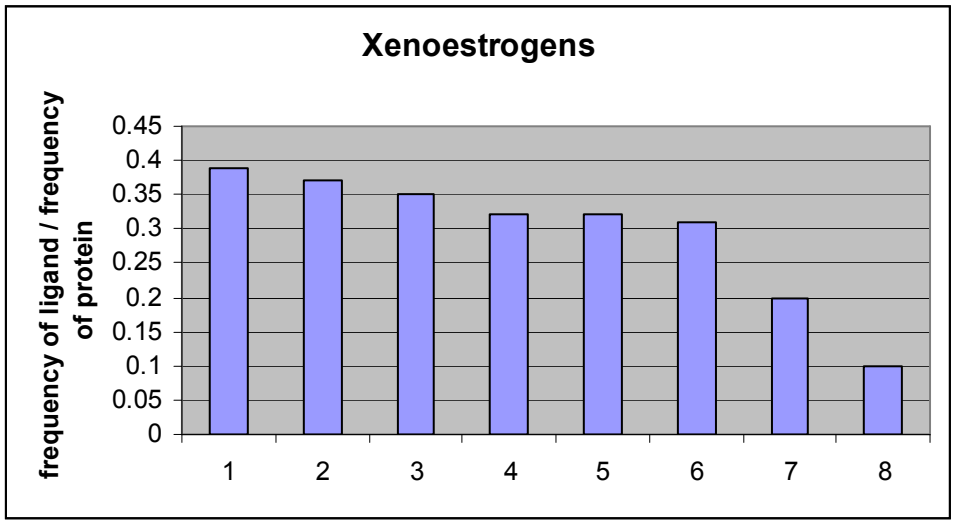

Figure 9. QCM Frequency Response to Ligand Binding. This graph represents the normalized frequency shifts from the QCM for ligand binding relative to the immobilization of HBD-C417 for two trials with each ligand. Ligand include: (1) estrone (2) apigenin (3) ergosterol (4) methoxychlor (5) octyphenol (6) baicalein (7) kaempferol (8) 2,4 dichlorophenoxyacetic acid. Experiments were done at concentrations of 20 μM ligand.

In addition to the binding capacity of the biosensor for a variety of ligands we tested the sensor to monitor its capability to bind 17-β-estradiol in the nanomolar range. Results are shown in Figure 10 which illustrate a logarithmic trend in the frequency shift with increasing concentrations and begins to plateau near the 20 μM range. It was thus postulated that a concentration of 20 μM 17β-estradiol was sufficient to saturate the majority of HBDC417 immobilized receptors. It is also important to notice that a significant reading was detected in the nanomolar range (100 nM). Subsequent trials with estradiol and other ligands including those shown above did not provide us with any further sensitivity. Thus our lowest limit of concentration for detection by this methodology with the Maxtec instrument is 100 nM. All studies with the HBDC530 mutant resulted in an even lower sensitivity. We surmise this because the residue 530 is located near the binding pocket and it may be assumed that the attachment to the gold surface does not allow the helix 12 to fully close to capture the ligand. In most of the studies with HBDC530 the ligand binds but after time is released from the protein. Figure 11 and Figure 12 depict these phenomena with estradiol and nonylphenol.

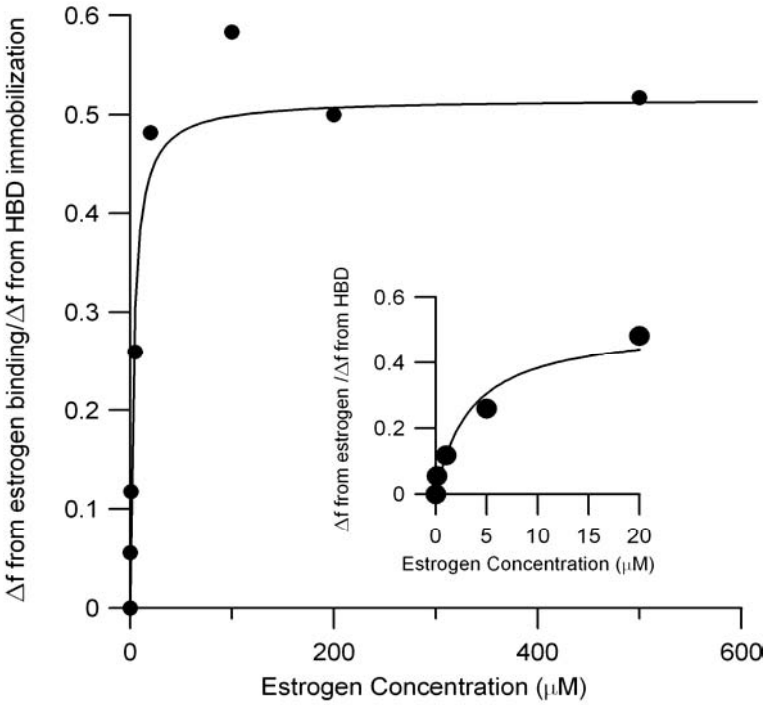

Figure 10. Graphical representation of the ligand frequency shift versus the17-β-estradiol (E_2) concentrations incubated at the surface of the HBDC417 immobilized receptors.

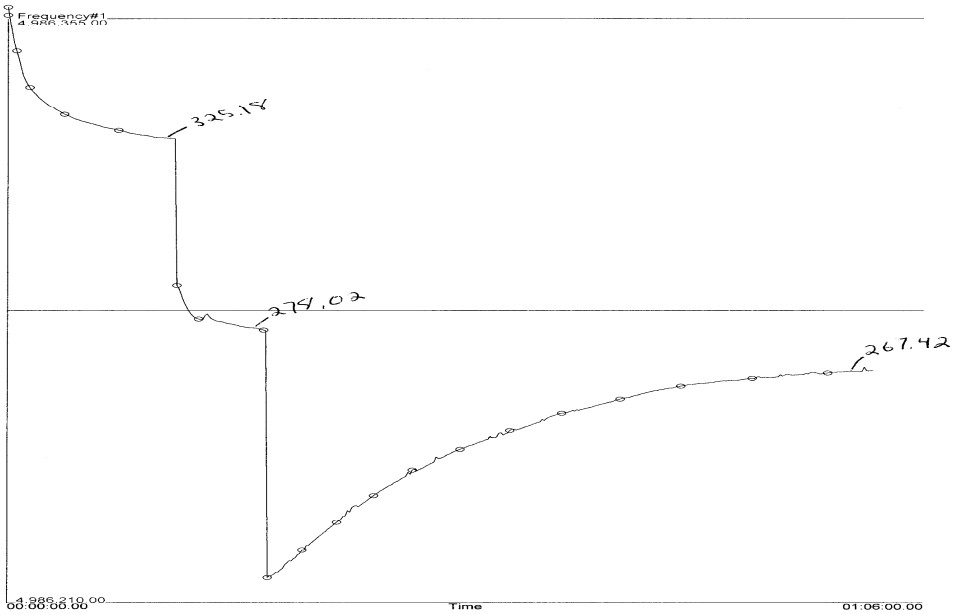

Figure 11. The Maxtec QCM experiment of HBDC530 and estradiol. Baseline was established at 325 Hz addition of protein caused a reduction of frequency of 47 Hz and the addition of 20 mM estradiol in buffer and ethanol gave an additional decrease in frequency of 10 Hz.

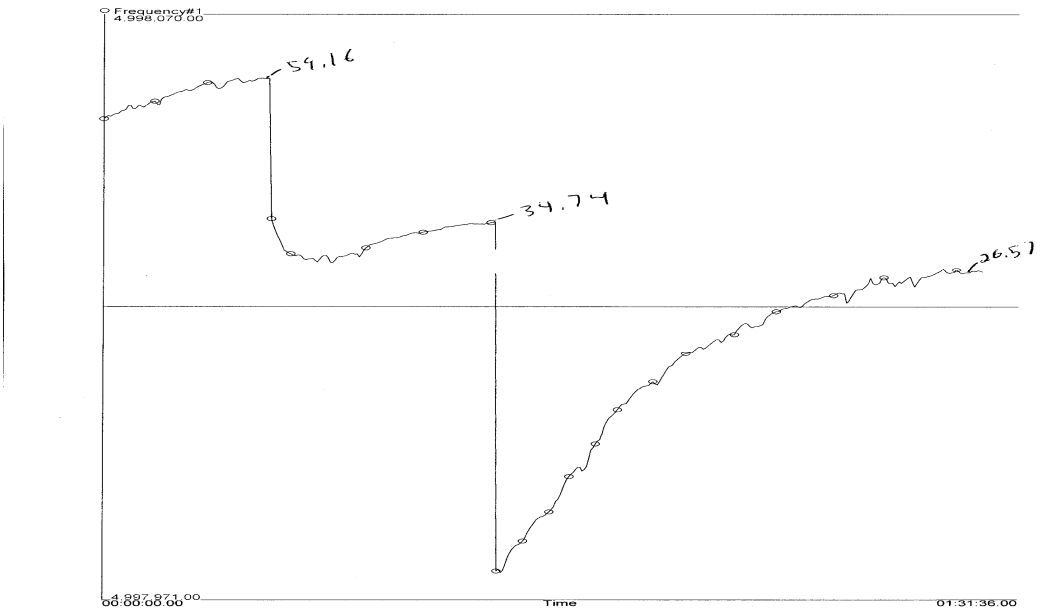

Figure12.. The Maxtec QCM experiment of HBDC530 and nonylphenol. Baseline was established and the addition of protein caused a reduction of frequency of 24 Hz and the addition of 20 mM nonylphenol in buffer and ethanol gave an additional decrease in frequency of 8 Hz. As you can observe the frequency is increasing with time. In subsequent experiments the frequency after 2 hours reached the frequency of the immobilized protein layer. This indicates that the protein is releasing the ligand.

We investigated the additive properties of ligands. In these experiments we incubated two ligands together on the quartz crystal. In all cases if we were above the concentration of detection 100 nM no significant difference in the QCM response was observed when two compounds were added together. Since our limit of detection is not low enough for environmental samples, we abandoned these experiments. A representative graph is shown for these types of experiments in Figure 13.

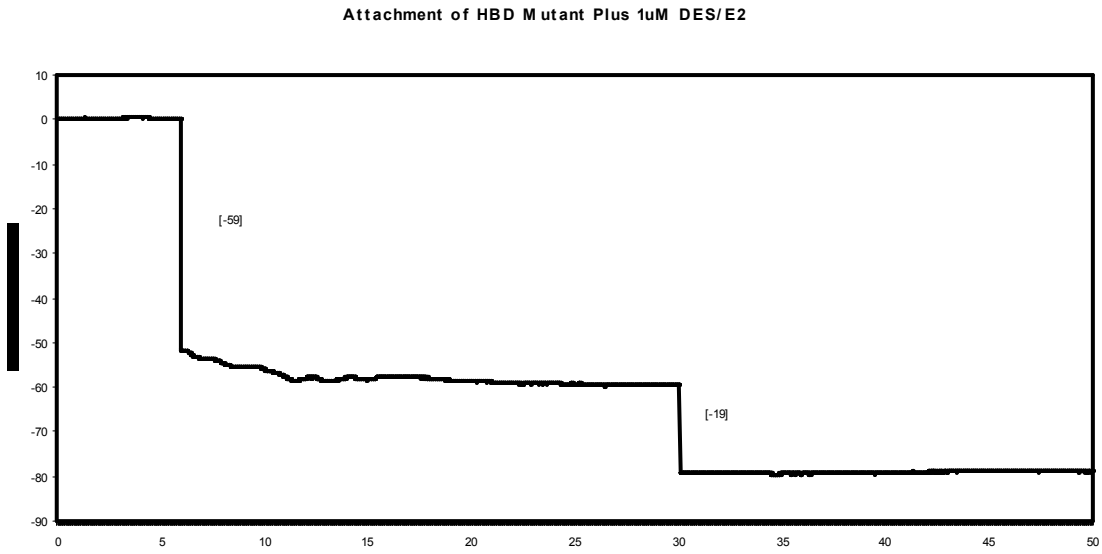

Figure 13 The combination of DES and estradiol as ligands in the Maxtec QCM experiment.

Studies relating to the direct attachment of the protein to the surface.
Our work has brought up many questions as to why the QCM responds in such a manner with proteins directly attached to the gold surface. In many other studies, researchers have attached proteins to linkers to passivate the surfaces. We wanted to examine the effect of immobilization strategy on the QCM frequency response to ligand binding experienced by HBD. The thiol linker 3,3-dithiobis [N-(5-amino-5-carboxypentyl)-propionamide-N'-N'-diacetic acid] complexed with nickel (Ni-NTA) was used as a means to immobilize the genetically engineered ligand binding domain of the estrogen receptor. The thio end of the linker binds to the gold surface via a gold-sulfur bond and provides a self-assembled monolayer on the gold. The Ni-NTA chelate end which is commonly used for histidine-tagged protein purification or separation, binds to the genetically engineered binding domain of the estrogen receptor. In this study the frequency response to 17β-estradiol is compared for the receptor directly immobilized on the gold surface to receptor immobilized via a Ni-NTA linker. The details of this study are in the appendix in the paper: Baltus, R.E, Carmon, K.S.,and Luck, L.A.(2007) Quartz Crystal Microbalance with Immobilized Protein Receptors: A Comparison of Response to Ligand Binding for Direct Protein Immobilization and Protein Attachment via a Disulfide Linker. *Langmuir* **23** 3990-3995.

Studies of the HBD with the Q-Sense Instrument
Experiments with HBDC417 and HBDC530 were performed at McGill University under the direction of Dr. Nathalie Tufenkji. This system allows 4 simultaneous experiments to be performed under flow conditions. The following experiment shows HBDC417 immobilization and subsequent incubation with the ligand nonylphenol (5MM in 90% ethanol).

The configuration was at follows:

Cell 1: Ligand + Buffer, Cells 2 & 3: HBD+ Ligand, Cell 4: HBD + Buffer.

Procedure:

1. TG Buffer was pumped until baseline was achieved.
2. A total volume of 1 ml of HBD dissolved in Buffer was injected in cells 2, 3 & 4.
3. The pump was halted and an incubation period of 1 hr was allowed.
4. The ligand (4-Nonylphenol) was injected in cells 1, 2 & 3 @ 5 *m*M.
5. The pump was stopped followed by an incubation period of 15 min. **There is no frequency change observed when ligand is added to the protein.**
6. The system is rinsed with buffer solution, and the frequency shift returns to the previous levels
7. The protein binds to the gold surface
8. It appears that the nonylphenol may bind to the gold surface as well

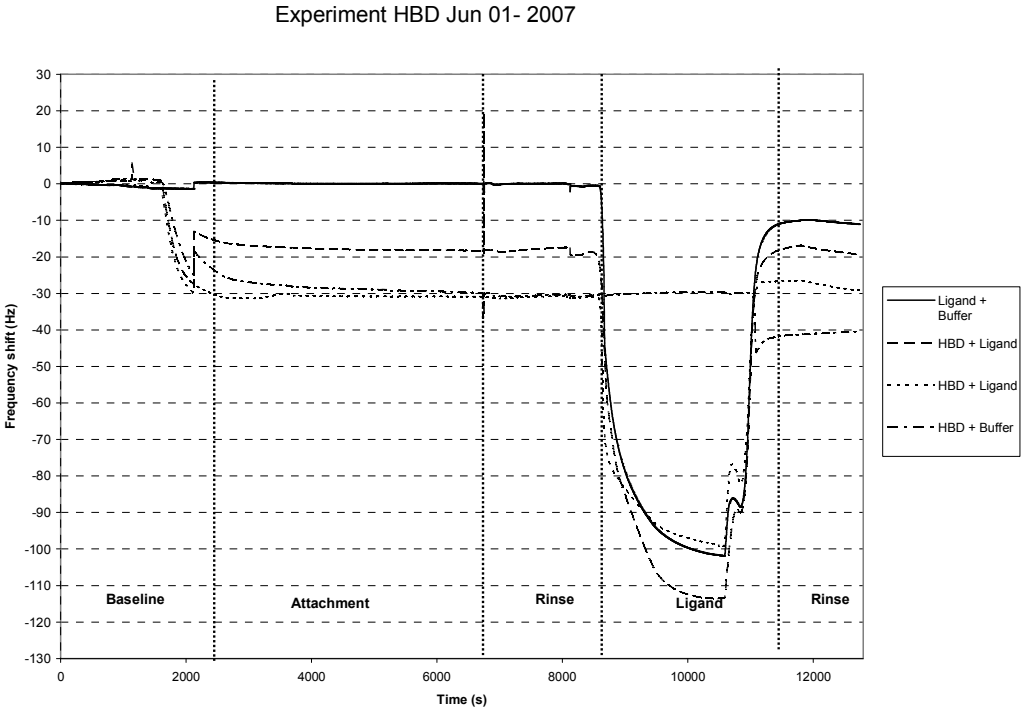

Figure 14. The Q-sense experiment with HBDC417 described above.
The Q-sense and Maxtec instruments showed a 50 to 60 Hz change when the proteins (both HBDC417 and HBDC530) were added. The Q-sense instrument showed a decrease in frequency along with an increase in the dissipation as the protein deposits on the surface. Experiments with both mutants of HBD using other iterations failed to show a change in frequency when ligand (estradiol, nonylphenol, estrone) were added. A number of trials were done with the three estrogenic compounds and proteins.

We also tried to repeat experiments on the glucose and galactose binding protein which showed in the Maxtec experiments a large frequency shift upon ligand addition. These

glucose experiments with the Q-sense instrument also did not parallel those of the Maxtec instrument. Both Maxtec and Q-sense representatives have been consulting with our two groups on this dilemma. It appears that we are not the only ones who are having these discussions. There seems to be a large disconnect between the technologies and the proprietary nature of these companies have not made these studies transparent. Although this course has not been productive in terms of developing a method for capturing new ligands, it has opened new doors for scientific inquiry. We plan to pursue this challenge in the next few months by further study in the area of surface phenomena with proteins. Dr. Luck's group plans to beta test a new QCM by Sierra Sensors and the Tufenkji group is beta testing a new Q-sense instrument with the estrogen receptors made for this project.

While investigating the predicament mentioned, above we decided to test a number of compounds that were used in the purification of the protein to see if they might be interfering with the Q-sense instrument. One such compound was imidazole. This compound is used to isolate the protein by competing with the His tagged protein for the NTA on the purification column. It is also present in μM quantities in the final preparation used in the QCM experiments. Our experiments showed in both the Q-sense and the Maxtec that imidizole does not bind to the gold significantly under 5 mM.
We also tested DNA to see if it may bind to the surface. The reasoning for this is that the preps may vary from time to time and one of the key differences is the isolation of the protein from the cell contents. DNA many times contaminates protein preps. Our conclusion from data from the Maxtec instrument is that DNA does not bind to the gold surface.

Humic Acid Studies
In screening waste water for unidentified EDCs we needed to assess whether the dissolved organic matter (DOC) content of the solutions would be of concern. We used a standard river humic acid standard (International Humic Substances Society, Suwanee River Humic Acid) as a model compound for this study. We made solutions of the standard organic matter in buffer solutions to see if the organics would bind to the gold crystal and interfere with binding of proteins to the surface. We also need to test this organic matter on gold surface for work that we may pursue with gold nanoparticles. Both QCM instruments were used for these studies. In both experiments, our results indicate that DOC levels that are occurring in sewage samples are not likely to bind to the gold surfaces. We see an ~ -2 Hz shift in the Q-sense experiment of the humic acid at 100 mg/L which is likely to be the highest concentration that would occur in samples of interest. Concentration of 20 mg/L and 1 mg/L show no significant frequency decrease in comparison to the buffer. Studies with the Maxtec instrument show no changes in frequency upon subsequent addition of humic acid up to 50 mg/L in the glass cell apparatus. These experiments were done over a 7 hour period.

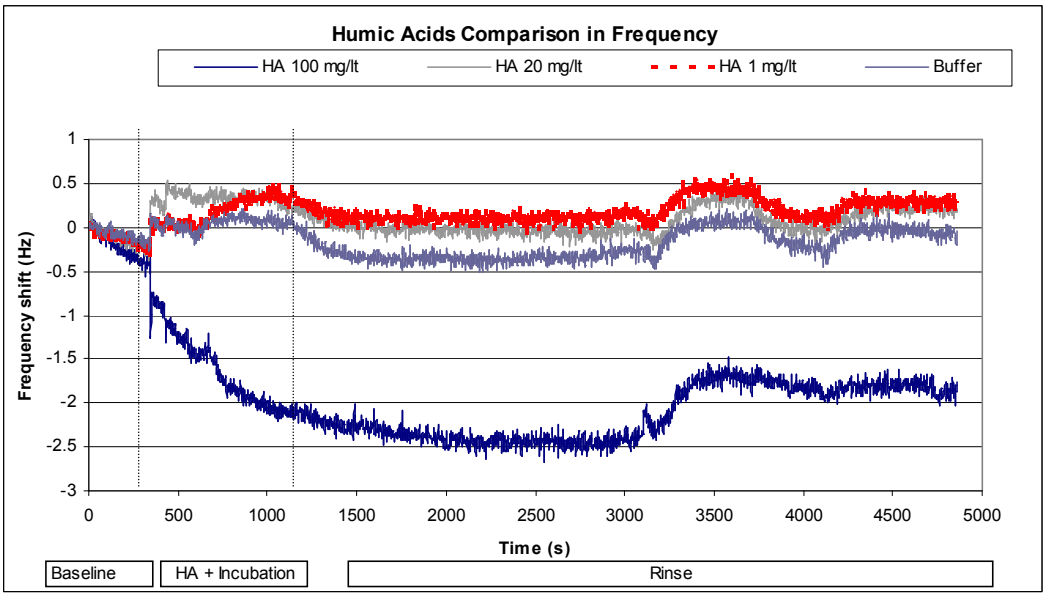

Figure 15. Experiments with the Q-Sense instrument using 4 crystals. After a baseline was established addition of each sample of humic acid was added by flow mechanism. An incubation of 10 minutes was used. Crystals were rinsed after the incubation.

Investigation of the gold nanoparticles for trapping EDCs
Since our QCM experiments were not sensitive enough to detect estrogens at low concentration, we started preliminary work on the development of surface-immoblized proteins on gold nanoparticles with detection of ligand binding by an electrochemical system that is known to be more sensitive. Our first studies have been done with the glucose and galactose binding protein which has been our model system due to the protein being readily available and stable. The investigation of the nanoparticle sensor showed detection in the range of the glucose receptor. The manuscript attached in the appendix gives the details of the experiments and methodology.

Key Research Accomplishments

- ♦ Established that the direct attachment of the protein to the gold surface is key to the QCM experiments.
- ♦ Showed that Q-Sense and Maxtec QCM Instrumentation does not illustrate the same responses for ligand binding.
- ♦ Showed that humic acid does not bind to the gold so all experiments done on gold surfaces will be viable with environmental samples containing high levels of dissolved organic matter
- ♦ Showed the sensitivity of the QCM is not yet good enough to be used in environmental studies of estrogenic substances present at low concentrations

- ♦ Showed electrochemical detection of ligand binding by nanoparticles may be a more viable methodology for EDC detection

Reportable Outcomes

Manuscripts

Andreescu, S. and Luck, L.A. (2007) Genetically Engineered Protein Films on Gold Nanoparticles: A Novel Electrochemical Glucose Biosensor in press *Analytical Biochemistry*

Baltus, R.E, Carmon, K.S.,and Luck, L.A.(2007) Quartz Crystal Microbalance with Immobilized Protein Receptors: A Comparison of Response to Ligand Binding for Direct Protein Immobilization and Protein Attachment via a Disulfide Linker. *Langmuir* **23** 3990-3995.

Roy, U. and Luck, L.A. (2007) Molecular Modeling of the Estrogen Receptor Using Molecular Operating Environment. *Biochemistry and Molecular Biology Education* **35** 238-243.

Abstracts

Luck, L.A., Layhee, A. W., Abramowitz, D.J., Standley, L.J., and Rudel, R.A. Genetically Engineered Protein Films on the Quartz Crystal Microbalances: A Biosensor for the Detection of Xenoestrogens 235th ACS National Meeting, New Orleans, LA April 2007 accepted

Luck, L.A. and Andreescu, S. Genetically Engineered Protein Films on Gold Nanoparticles: A Novel Electrochemical Glucose Biosensor VII European Symposium of the Protein Society. Stockholm/Uppsala Sweden, May 2007

Luck, L.A , Carmon, K.S., and Baltus, R.E. Detection of Small Ligands using a Quartz Crystal Microbalance with Genetically Engineered Proteins. 1st Annual International QCM-D Conference. Boston MA December 2006

Luck, L.A , Carmon, K.S., and Baltus, R.E. Development of a QCM Biosensor using Genetically Engineered proteins. 34th NERM Meeting of the ACS. Binghamton, NY October 2006 (no abstract)

Sokolov, I., Luck, L.A. and Subba-Rao, V. Change in Rigidity in the Glucose/Galactose Receptor Detected with AFM: A Phenomenon that will be Key to the Development of a Family of Biosensors. 34th NERM Meeting of the ACS. Binghamton, NY October 2006 (no abstract)

Luck, L.A. Biosensors Using Genetically Engineered Proteins: Incorporating Undergraduates in Interdisciplinary Research Projects in the Biosensor Field. 20th Symposium of the Protein Society, San Diego, CA August 2006

Students Trained

Graduate Students

Kendra Carmon
Jessica King

Undergraduate Students

Robert Byno BS Chemistry 2007 will be grad student Jan 08
Kathryn Whipple Bs Chemistry 2007
Dave Abramowitz BS Biochemistry 2007
Adam Layhee (supported by grant)
Courtney Sipe sophomore
Jeremy Childs transferred to UB (supported by grant)
Candace Moulton sophomore

Funding applied for
NSF MRI grant for mass spectrometer Co PI with Guissepi Petrucci, chemistry department at the University of Vermont

Conclusions

This concept award was granted to develop a biosensor for identifying novel endocrine disrupting chemicals. We proposed to develop a QCM-biosensor that would be able to sense and identify estrogenic activity in complex mixtures. The initial biosensor has promise for this capability but our subsequent studies have shown that the QCM biosensor will not have the sensitivity to sequester and release estrogens that are in low concentration. Our work has also pointed to a discrepancy between two different types of instruments, the Maxtec and the Q-Sense instrument. The Maxtec shows a response for ligands whereas the Q-Sense instrument which is touted to be more sensitive does not. This study has raised a number of questions in the QCM field that will open doors for much research in the future. We have clearly demonstrated that humic acid as a model for dissolved organic substances in wastewater and other sources did not interfere with the gold surfaces used in a number of electrochemical methods. We also have shown that electrochemical methods in combination with gold nanoparticles may be a more sensitive methodology for ligand capture for EDCs.

References

1. Reiter, L. W., DeRosa, C., Kavlock, R. J., Lucier, G., Mac, M. J., Melillo, J., Melnick, R. L., Sinks, T., and Walton, B. T. (1998) The U.S. Federal Framework for Research on Endocrine Disruptors and an Analysis of Research Programs Supported During Fiscal Year 1996. *Environ. Health Persp. 106*, 105-113.

2. Crews D., Willingham E., and Skipper J. K. (2000) Endocrine Disruptors: Present Issues, Future Directions *The Quarterly Review of Biology 75*, 243-259.
3. Shelby, M. D., Newbold, R. R., Tully, D. B., Chae, K., and Davis, V. L. (1996) Assessing Environmental Chemicals for Estorgenicity using a Combination of in vitro and in vivo Assays *Environ. Health Persp. 104*, 1296-1300.
4. Katzenellenbogen, B. S., Montano, M. M., Ediger, T. R., Sun, J., Ekena, K., Lazennec, G., Martini, P., McInerney, E. M., Delage-Mourroux, R., Weiss, K., and Katzenellenbogen, J. A. (2000) Estrogen Receptors: Selective Ligands, Partners, and Distinctive Pharmacology *Recent Progress in Hormone Research 55*, 163-195.
5. Seielstad, D. A., Carlson, K. E., Kushner, P. J., Greene, G. L., and Katzenellenbogen, J. A. (1995) Analysis of the Structural Core of the Human Estrogen Receptor Ligand Binding Domain by Selective Proteolysis/mass Spectrometric Analysis *Biochemistry 34*, 12606-12615.
6. Janshoff, A., Galla, H. J., and Steinam, C. (2000) Piezoelectric Mass-Sensing Devices as Biosensors- An alternative to Optical Biosensors? *Angewandte Chemie 39*, 4004-4032.
7. Parker, M. G. (1993) Steroid and Related Receptors *Curr. Opin. Cell Biol. 5*, 499-503.
8. Shiau, A. K., Barstad, D., Loria, P. M., Cheng, L., Kushner, P. J., Agard, D. A., and Greene, G. L. (1998) The Structural Basis of Estrogen Receptor/coactivator Recognition and the Antagonism of this Interaction by Tamoxifen *Cell 95*, 927-937.
9. Brzozowski AM, Pike AC, Dauter Z, Hubbard RE, Bonn T, Engstrom O, Ohman L, Greene GL, Gustafsson JA, and Carlquist M. (1997) Human Estrogen Receptor Ligand-Binding Domain In Complex With Raloxifene *Nature 389*, 753-758.
10. Pike AC, Brzozowski AM, Hubbard RE, Bonn T, Thorsell AG, Engstrom O, Ljunggren J, Gustafsson JA, and M, C. (1999) Structure of the ligand-binding domain of oestrogen receptor beta in the presence of a partial agonist and a full antagonist. *EMBO 18*, 4608-4618.
11. Pike, A. C. W., Brzozowski, A. M., Walton, J., Hubbard, R. E., Thorsell, A., Li, Y., Gustafsson, J., and Carlquist, M. (2001) Structural Insights into the Mode of Action of a Pure Antiestrogen *Structure 9*, 145-153.
12. Brzozowski A. M., Pike A. C. W., Dauter Z., E., H. R., Bonn T., Engstrom, O., Ohman L., Greene G. L., Gustafsson J., and Carlquist M. (1997) Molecular Basis of Angonism and Antagonism in the Oestrogen Receptor *Nature 389*, 753-758.
13. Sokolov, I., Venkatesh, S., and Luck, L. A. (2006) Change in Rigidity in the Activated Form of the Glucose/ Galactose Receptor from E.coli: A Phenomenon That Will Be Key to the Development of Biosensors *Biophys. J. 90*, 1058-1063.
14. Carmon, K. S., Baltus, R. E., and Luck, L. A. (2005) A Biosensor for Estrogenic Substances Using the Quartz Crystal Microbalance *Anal. Biochem. 345*, 277-283.
15. Kumar, V., Green, S., Stack, G., Berry, M., Jin, J. R., and Chambon, P. (1987) Functional domains of the human estrogen receptor *Cell 51*, 941-951.
16. Katzenellenbogen, J. A., and Katzenellenbogen, B. S. (1996) Nuclear hormone receptors: ligand-activated regulators of transcription and diverse cell responses *Chemical Biology 3*, 529-536.

17. Brandt, M. E., and Vickery, L. E. (1997) Cooperativity and Dimerization of Recombinant Human Estrogen Receptor Hormone -binding Domain *The Journal of Biological Chemistry 272*, 4843-4849.
18. Gee, A. C., and Katzenellenbogen, J. A. (2001) Probing Conformational Changes in the Estrogen Receptor: Evidence for a Partially Unfolded Intermediate Facilitating Ligand Sinding and Release *Molecular Endocrinology 15*, 421-428.
19. Carlson, K. E., Choi, I., Gee, A., Katzenellenbogen, B. S., and Katzenellenbogen, J. A. (1997) Altered Ligand Binding Properties and Enhanced Stability of a Constitutively Active Estrogen Receptor: Evidence That an Open Pocket Conformation Is Required for Ligand Interaction *Biochemistry 36*, 14897-14905.
20. Seielstad, D. A., Carlson, K. E., Katzenellenbogen, J. A., Kushner, P. J., and Greene, G. L. (1995) Molecular Characterization by Mass Spectrmetry of the Human Estrogen Receptor Ligand-Binding Domain Expressed in *Escherichia coli Molecular Endocrinology 9*, 647-658.
21. Reese, J. C., and Katzenellenbogen, B. S. (1991) Mutagenesis of Cysteines in the Hormone Binding Domain of the Human Estrogen Receptor *The Journal of Biological Chemistry 266*, 10880-10887.
22. Baltus, R. E., Carmon, K. S., and Luck, L. A. (2007) Quartz Crystal Microbalance with Immobilized Protein Receptors: A Comparison of Response to Ligand Binding for Direct Protein Immobilization and Protein Attachment via a Disulfide Linker. *Langmuir 23*, 3990-3995.

Appendices

Available online at www.sciencedirect.com
ScienceDirect
Analytical Biochemistry xxx (2008) xxx–xxx
ANALYTICAL BIOCHEMISTRY
www.elsevier.com/locate/yabio

Studies of the binding and signaling of surface-immobilized periplasmic glucose receptors on gold nanoparticles: A glucose biosensor application

Silvana Andreescu [a,*], Linda A. Luck [b]

[a] Department of Chemistry and Biomolecular Science, Clarkson University, Potsdam, NY 13699, USA
[b] Department of Chemistry, State University of New York at Plattsburgh, Plattsburgh, NY 12901, USA

Received 21 November 2007

Abstract

Genetically engineered periplasmic glucose receptors as biomolecular recognition elements on gold nanoparticles (AuNPs) have allowed our laboratory to develop a sensitive and reagentless electrochemical glucose biosensor. The receptors were immobilized on AuNPs by a direct sulfur–gold bond through a cysteine residue that was engineered in position 1 on the protein sequence. The study of the attachment of genetically engineered and wild-type proteins binding to the AuNPs was first carried out in colloidal gold solutions. These constructs were studied and characterized by UV–Vis spectroscopy, transmission electron microscopy, particle size distribution, and zeta potential. We show that the genetically engineered cysteine is important for the immobilization of the protein to the AuNPs. Fabrication of the novel electrochemical biosensor for the detection of glucose used these receptor-coated AuNPs. The sensor showed selective detection of glucose in the micromolar concentration range, with a detection limit of 0.12 μM.

Keywords: Gold nanoparticles; Biofunctionalization; Periplasmic glucose/galactose receptor; Biosensor; Surface immobilization; Self-assembled protein monolayers

During the past decade, gold nanoparticles (AuNPs)[1] have attracted an enormous amount of attention in the scientific and engineering fields due to their multifaceted properties. Recently, they have been widely used in combination with proteins, peptides, enzymes, antibodies, and nucleic acids [1–10]. These biomolecule–AuNP assemblies have found applications in biotechnology, biology, and medicine for the development of biological assays and biolabeling, in drug delivery, and as probes in cancer detection. Immobilization of proteins in a functional state on AuNPs is of critical importance in practical applications, especially in biosensing and biolabeling [7–10].

Here we describe studies that incorporate genetically engineered periplasmic binding proteins that sense glucose on the surface of AuNPs. We further describe an electrochemical methodology to use these protein–AuNP assemblies for use in biosensors to detect glucose in the micromolar range. For the most part, biosensors use target molecules that are immobilized on or within a suitable material that is in direct contact with the surface of a transducer. AuNPs are an ideal platform for biosensors, especially for those with electrochemical detection, because the gold surface area is suitable for binding of biomolecules and the metal facilitates direct and fast electron transfer.

* Corresponding author. Fax: +1 315 268 6610.
E-mail address: eandrees@clarkson.edu (S. Andreescu).

[1] *Abbreviations used:* AuNP, gold nanoparticle; GGR, glucose/galactose receptor; GGR–WT, glucose/galactose receptor–wild type; GGR–Cys, glucose/galactose receptor where alanine was replaced by cysteine at the N-terminal position; ζ-potential, zeta potential; PSD, particle size distribution; TEM, transmission electron microscopy; PB, phosphate buffer; DI, deionized water; HR–TEM, high-resolution JEOL 2010 transmission electron microscopy; GCE, glassy carbon electrode; SEM, scanning electron microscopy; CV, cyclic voltammetry.

0003-2697/$ - see front matter © 2007 Elsevier Inc. All rights reserved.
doi:10.1016/j.ab.2007.12.035

Moreover, the AuNPs, as compared with flat gold surfaces, have a much higher surface area, allowing the loading of a larger amount of protein and potentially more sensitivity [7–10]. For many biosensor applications in the literature, the biomolecules are attached to gold surfaces via thiol linkers attached on the gold surface [11,12] or, as in the current study, are directly linked to the gold by the use of sulfur atoms within the bioentity [13,14]. The receptors used in a number of studies from our laboratories have used a cysteine residue endogenous to the native protein, or one that is genetically engineered into the protein can be used to link and spatially orient the biomolecule on the gold surface [15–22]. When a surface-exposed cysteine residue on a protein is not feasible, thiol linkers to other residues on a protein allow semispecifically oriented layers on the surface [23]. Although there has been some discussion in the literature pointing to protein deposition without exposed cysteines, a number of studies from our laboratories have indicated that native glucose/galactose receptors (GGRs) without a genetically engineered cysteine residue do not bind to the gold surface, whereas receptors with a surface-exposed cysteine form a stable affinity bond to gold surfaces [15–22].

The current study was undertaken to explore the oriented immobilization of receptor proteins to AuNPs. For our purposes of developing a glucose biosensor, we used the periplasmic glucose/galactose receptor–wild type (GGR–WT), which is highly specific for its natural cognate ligands. Ligand binding is accompanied by a large conformational change [15]. GGR–WT has no native cysteines, but we have developed a number of mutants that have one surface-exposed cysteine residue that can be used to attach the protein to a gold surface. For this study, we used the mutant where alanine was replaced by cysteine at the N-terminal position (GGR–Cys). This engineered site provides an SH group for protein linkage to the gold surfaces. The advantage of such an approach is the precise control and orientation of the protein on the electrode surface with the preservation of its functional properties. This system circumvents the denaturation or instability problems commonly encountered when immobilization is achieved through physical adsorption or covalent linkage of natural proteins.

A number of studies have been reported using the GGR and genetically engineered cysteine mutants of this receptor where we have looked at detected binding through changes in surface plasmon resonance [17], frequency decrease on a quartz crystal microbalance [15], change in rigidity by atomic force microscopy [22], and electrochemical impedance [18,21]. In the current study, the AuNPs with immobilized receptor proteins are characterized by UV–Vis spectroscopy, zeta potential (ζ-potential), particle size distribution (PSD), and transmission electron microscopy (TEM). We demonstrate the utility of these AuNPs as a means to detect glucose in the micromolar range. In addition, this study serves as a model for the development of electrochemical biosensors using receptors that bind to small molecules. Applicability of this system could be extended to a number of protein families, including the steroid hormone receptor superfamily, and to the detection of xenoestrogens.

Materials and methods

Expression and purification of recombinant proteins

The preparation and expression of GGR–WT and GGR–Cys have been described previously [17]. Fig. 1 illustrates the position of the amino acid cysteine mutation and the orientation of the protein on the nanoparticle.

Reagents and solutions

$HAuCl_4$ $3H_2O$ (23.03 wt% Au, 6.5 wt% free HCl) was purchased from Degussa (South Plainfield, NJ, USA). Isoascorbic acid ($C_6H_8O_6$) was obtained from Fluka. The phosphate buffer (PB) solution (pH 6.5) used for the preparation of 10 mM $K_3[Fe(CN)_6]$ (Fischer Scientific, Fair Lawn, NJ, USA) contains 0.1 M KH_2PO_4 (Fischer Scientific) and 0.1 M Na_2HPO_4 (J. T. Baker, Phillipsburg, NJ, USA). All aqueous solutions were pre-

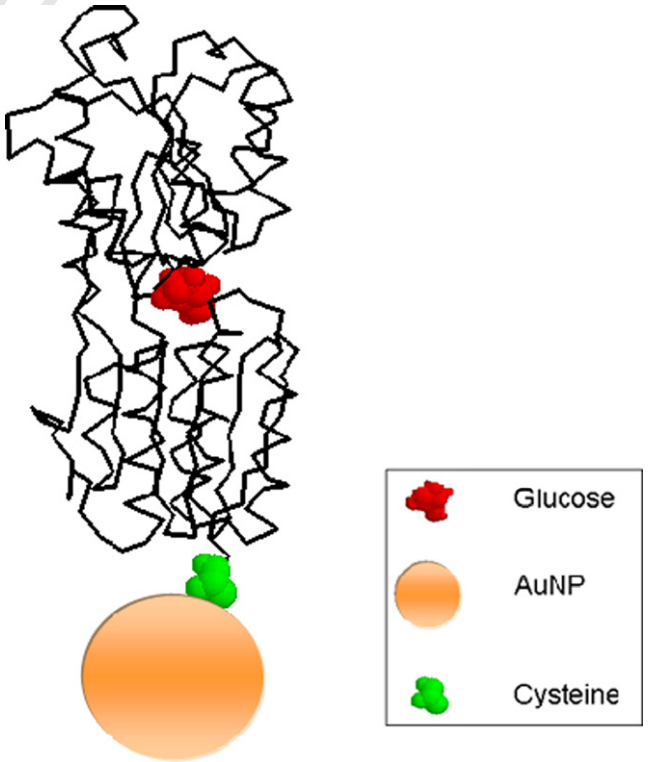

Fig. 1. Backbone structure of the glucose and galactose binding protein attached to the AuNP. This figure illustrates the position of the alanine to cysteine mutation at position 1 in green and the glucose in the binding pocket in red. The drawing was done using PDB file 2GBP from the Protein Data Bank. The nanoparticle is not drawn to scale because it actually is 10 times larger than the protein. (For interpretation of the references to color in this figure legend, the reader is referred to the Web version of this article.)

Please cite this article in press as: S. Andreescu, L.A. Luck, Studies of the binding and signaling of surface-immobilized ..., Anal. Biochem. (2008), doi:10.1016/j.ab.2007.12.035

pared with deionized water (DI) using a Millipore Direct-Q system with a resistivity of 18.2 MΩ. D-Glucose, fructose, L-valine, and L-leucine were purchased from Sigma. Protein buffer contained 100 mM KCl, 10 mM Tris (pH 7.1), and 0.5 $CaCl_2$ (Tris buffer). Tris buffer was used in all experiments involving colloidal gold in the presence/absence of proteins.

Instrumentation

The UV–Vis spectra of AuNPs were recorded with a Shimadzu P2041 spectrophotometer equipped with a 1-cm path length cell. The electrokinetic properties, ζ-potential, and PSD were measured with a Brookhaven Zeta Plus–Zeta Potential Analyzer at 25 °C and calculated with standard software. The size, size distribution, and morphology of the AuNPs were measured by high-resolution JEOL 2010 transmission electron microscopy (HR–TEM).

All electrochemical measurements were performed with a PARSTAT 2263 electrochemical analyzer (Princeton Applied Research) equipped with Power Suite software. These electrochemical experiments were carried out using a conventional cell operating with an Ag/AgCl/3M NaCl as reference electrode, a platinum wire as counterelectrode, and a glassy carbon electrode (GCE) with a geometrical surface area of 28 mm^2 as working electrode. The cell and electrodes all were provided by Bioanalytical Systems (West Lafayette, IN, USA).

Preparation of gold colloids

Gold colloids were obtained by reduction of gold ions with isoascorbic acid as described previously [24]. All glassware used in the preparation of AuNPs was cleaned in an HNO_3 bath, rinsed thoroughly with distilled water, and dried prior to use. A stable red gold colloidal solution was obtained. The resulting AuNPs are uniform and highly dispersed, with an average particle diameter between 30 and 40 nm (as determined by TEM and scanning electron microscopy [SEM] analysis) [24]. The absence of dispersing agents during the preparation procedure ensures a clean gold surface, making them attractive for further modification with biomolecules.

Preparation of protein–AuNP conjugates: Study of protein attachment

The protein production and genetic engineering of the native glucose and galactose protein and the mutant used in this study were described previously [17]. For the current article, we have defined the native protein as GGR–WT and the alanine to cysteine mutant of GGR as GGR–Cys. An illustration of the position of this mutation and its binding on an AuNP is given in Fig. 1. The point of attachment of the cysteine residue is far from the glucose binding site in the GGR protein; thus, this modification has no effect on its binding capability.

The immobilization of both GGR–WT and GGR–Cys to the AuNPs was accomplished by mixing 0.84 ml of 0.2 mM colloidal gold solution with 0.14 ml of 7 μM protein solution. The solutions were stirred for approximately 20 to 30 s and then analyzed by UV–Vis spectroscopy and ζ-potential. The results were compared with the spectra of a control colloidal gold solution in the absence of protein. To evaluate the immobilization of the proteins on the AuNPs, the conjugates were separated by centrifugation (15 min at 6000 rpm) and the UV–Vis spectrum of the supernatant was recorded to check for the presence of proteins. For HR–TEM analysis, one drop of gold or protein-modified AuNP colloidal solution without sonication was deposited on a TEM copper grid and dried under vacuum.

Electrode preparation and electrochemical studies

AuNPs were electrodeposited on the surface of a GCE by electrodeposition from a gold solution. The procedure involves applying a constant potential of −200 mV for 60 s in a solution of 1.2 μM $HAuCl_4$. The solution was prepared in distilled water and deoxygenated by purging with N_2 for approximately 15 min. Prior to deposition, the GCE was cleaned and dried according to the following sequence: polish with 0.3 μm alumina powder, wash ultrasonically for 10 min in distilled water, rinse with distilled water, and dry under a nitrogen stream. The surface of the electrode prior to and after deposition of proteins was characterized by cyclic voltammetry (CV) using the model reversible redox couple $Fe^{II}(CN)_6^{4-}/Fe^{III}(CN)_6^{3-}$. For this purpose, the three electrodes were immersed in a classical electrochemical cell containing $K_3Fe(CN)_6$, 10 mM was prepared in PB (pH 6.5), and the potential was scanned between 0 and 0.6 V versus Ag/AgCl reference electrode at a scan rate of 50 mV/s.

Biosensor fabrication and binding studies

The GCE–AuNP electrodes prepared by electrochemical deposition were incubated in 0.5 ml of 7 μM GGR–WT (or GGR–Cys) for 1 h at room temperature. The electrodes were rinsed thoroughly with Tris buffer to remove the excess of unbound protein and were incubated in D-glucose solution at a given concentration. D-Fructose, L-valine, and L-leucine were used as negative controls because they are not natural ligands and do not bind to the protein. Protein immobilization, as well as the binding of target ligands, was evaluated by CV using $Fe(CN)_6^{3-}/Fe(CN)_6^{4-}$ solution (10 mM) in PB (pH 6.5) by scanning the potential between 0 and 0.6 V at a scan rate of 100 mV/s. For evaluation of nonspecific absorption of the protein, attachment of GGR–WT and subsequent binding of glucose were performed under the same experimental conditions as for GGR–Cys.

Please cite this article in press as: S. Andreescu, L.A. Luck, Studies of the binding and signaling of surface-immobilized ..., Anal. Biochem. (2008), doi:10.1016/j.ab.2007.12.035

Results and discussion

Study of binding and activity of recombinant proteins on AuNPs

UV–Vis spectroscopy

It is known that highly dispersed gold colloids (single particles) in solution present a single absorption peak attributed to quadrupole plasmon excitation [25]. The position of the plasmon absorption band depends on the size, surface properties, mutual interactions in the dispersion medium, and extent of aggregation. The attachment of the proteins on AuNPs and the surface changes due to the absorbed proteins are expected to affect the surface plasmon. This results in a color change in the solution [26]. Aggregation of AuNPs usually is observed as a red shift in the color arising from the absorption bands at long wavelengths due to coupling between plasmons of neighboring particles inside the aggregates. In general, the smaller the interparticle distance, the larger the red shift [27].

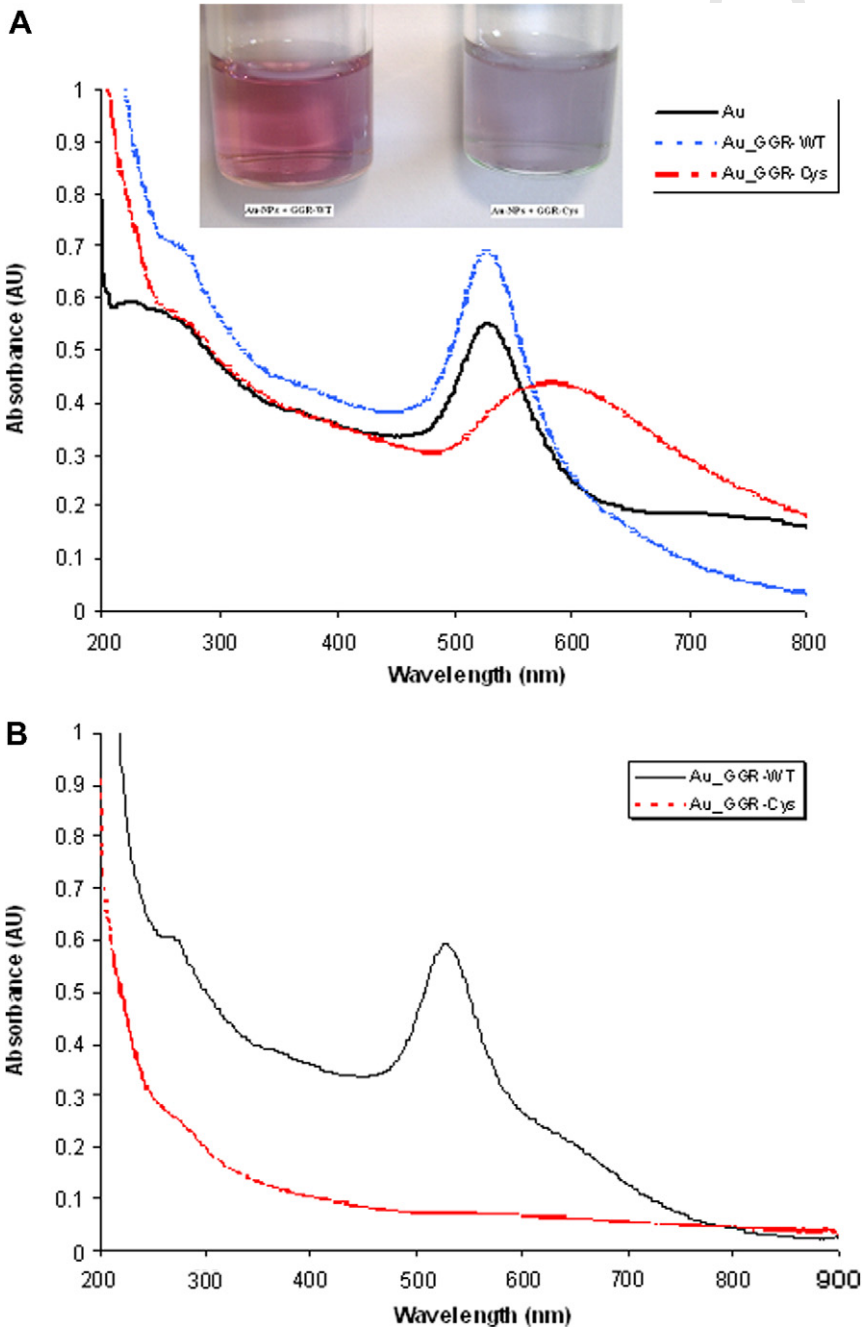

Fig. 2. UV–Vis spectra of AuNPs in the absence (Au) and presence of GGR–WT (Au_GGR–WT) and GGR–Cys (Au_GGR–Cys) immediately after mixing (A) and after 48 h incubation (B). In all experiments, a 10-mM Tris buffer solution (pH 7.1) containing 100 mM KCl and 0.5 mM $CaCl_2$ was used. Q3 Panel A inset: Color of gold sols in the presence of GGR–WT and GGR–Cys. AU, arbitrary units.

Please cite this article in press as: S. Andreescu, L.A. Luck, Studies of the binding and signaling of surface-immobilized ..., Anal. Biochem. (2008), doi:10.1016/j.ab.2007.12.035

The gold sols prepared in our preparations of Au^{3+} with isoascorbic acid have a red wine color and a well-defined absorbance peak at approximately 523 nm [24]. The stability of these electrostatically stabilized sols is highly dependent on the ionic strength of the system. Because very small additions of salts might cause coagulation of the AuNPs, we first studied the effect of the Tris buffer solution (pH 7.1) in which the proteins were prepared on the UV–Vis spectrum. The spectrum presents a well-defined peak at approximately 523 nm and a small wide shoulder starting at approximately 650 nm (Fig. 2A). The small peaks at approximately 226 and 320 nm are attributed to the square planar $AuCl_4^-$ complex ion. This spectrum was used as a control in the absence of proteins.

In the presence of proteins, gold colloidal particles form aggregates. On protein binding, the absorbance usually shifts to higher wavelength as the aggregation proceeds [24,25]. In our experiment, in the presence of GGR–WT, there was an increase in the gold peak at 523 nm, concomitant with the appearance of a new peak at 280 nm corresponding to the protein (Fig. 2A). No color change in the gold sols was observed. Thus, the wild-type protein does not bind to the gold particles.

In the presence of GGR–Cys, the color of the gold sol turned from red to blue, suggesting aggregation of the AuNPs due to the immobilized protein on their surface. The UV–Vis spectrum of the gold sols containing 1 μM GGR–Cys shows very distinct characteristics, with the peak corresponding to the AuNPs at 523 nm shifting to 600 nm and the new peak being significantly broader (Fig. 2A). In addition, there was no noticeable peak at 280 nm, suggesting that all of the protein in solution is attached to the AuNPs. The protein coating of the gold particles induces aggregation between the AuNPs, thereby producing changes in the plasmon absorption band associated with the color change.

The GGR–WT and GGR–Cys have distinctly different effects on the AuNPs that are more evident after 24 h of incubation of AuNPs and protein. After this time, the color of the solution and the characteristics of the UV–Vis spectrum of the GGR–WT did not change significantly. In contrast, the mixture of GGR–Cys and the AuNPs formed visible bluish aggregates that precipitated, leaving the supernatant nearly colorless. The UV–Vis spectrum in Fig. 2B illustrates this phenomenon. After centrifugation and separation, no protein was present in the supernatant in the case of GGR–Cys, suggesting that all of the protein was attached on the nanoparticles that formed large aggregates. Our spectrophotometric measurement showed that the total amount GGR–WT was retrieved in the supernatant, proving that the wild-type protein without the genetically engineered cysteine did not bind to the AuNPs under our experimental conditions.

ζ-Potential and TEM analysis

HR–TEM and ζ-potential analysis was used to characterize the surface properties, morphology, and size distribution of the AuNPs with and without immobilized protein. The surface modification can affect the surface charge of nanoparticles; this determines the dispersion and/or aggregation of colloidal solution at a given pH value. The bare AuNPs used in this work were negatively charged, with

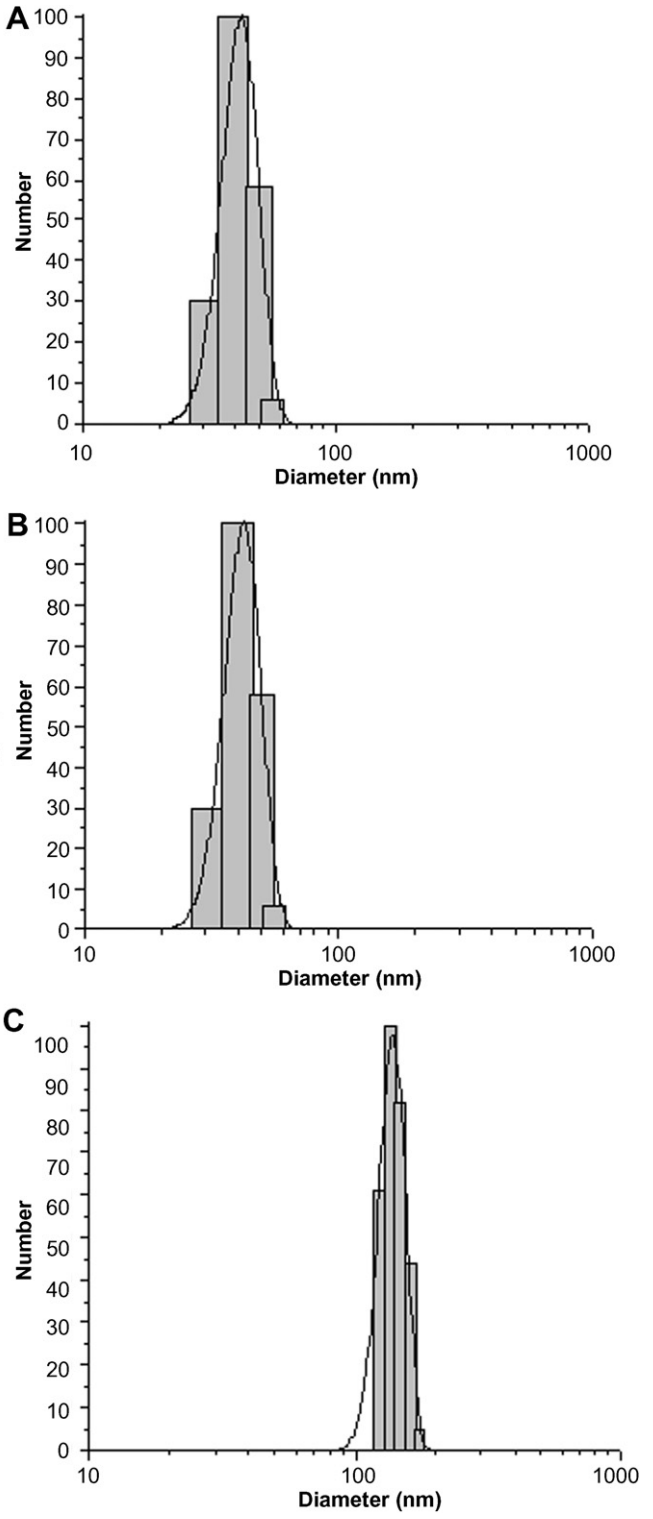

Fig. 3. PSD of AuNPs in the absence (A) and presence of GGR–WT (B) and GGR–Cys (C).

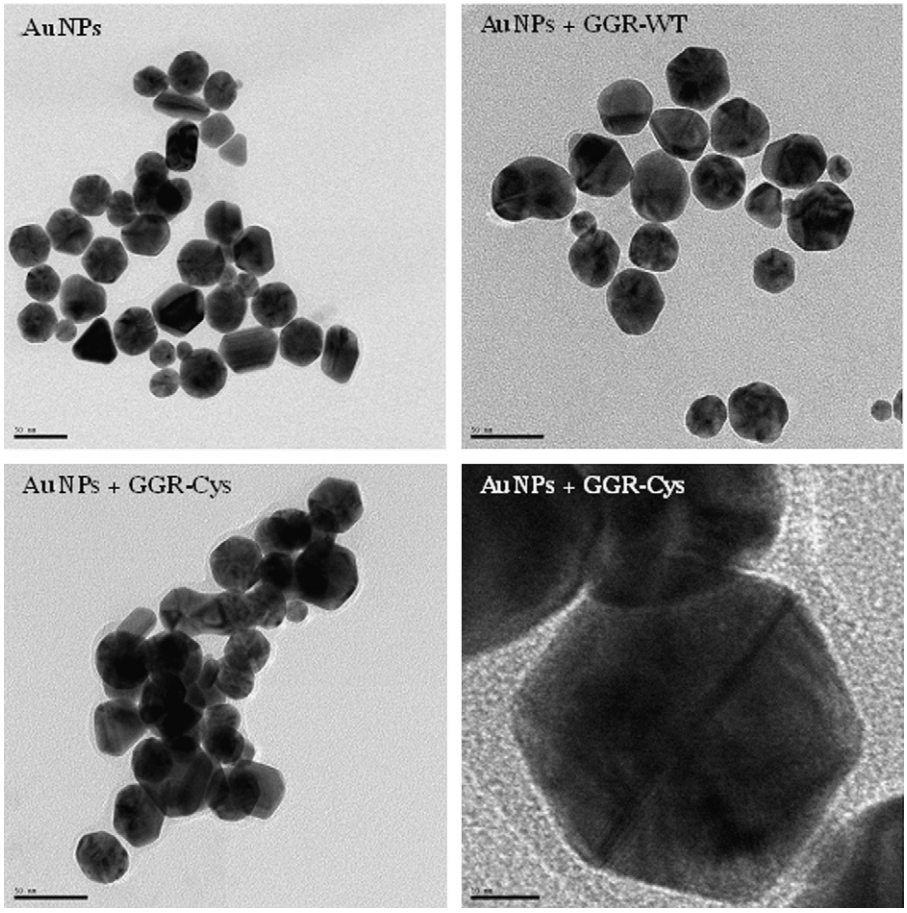

Fig. 4. TEM of AuNPs in the absence and presence of GGR–WT and GGR–Cys (scale = 50 nm). Different magnifications are shown for GGR–Cys (50 and 5 nm).

Table 1
Spectroscopic and morphological characteristics of AuNPs and AuNPs in the presence of GGR–WT and GGR–Cys

	ζ-Potential (mV)	Average size (nm)	UV–Vis peaks (nm)	Color/aggregation
AuNPs (Tris buffer)	−43.5 ± 4.1	42.5	523, 226, 320, and 650 (wide shoulder)	Red wine/Monodispersed particles
AuNPs + GGR–WT	−19.3 ± 2.0	59.4	523 and 280	Red wine/Monodispersed particles
AuNPs + GGR–Cys	−4.2 ± 6.6	139.6	600 (wide peak)	Blue/visible aggregates

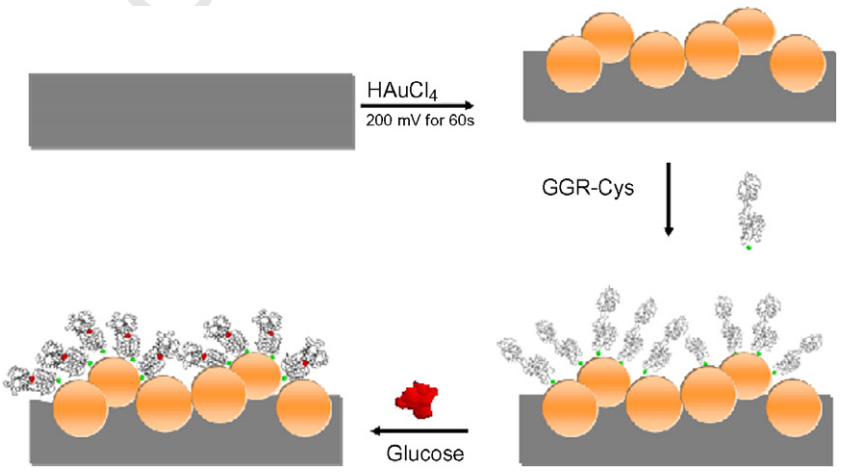

Fig. 5. Fabrication steps of the GCE–AuNP glucose sensor illustrating the binding of the protein via the cysteine residue on the GGR–Cys receptor and the subsequent glucose binding.

Please cite this article in press as: S. Andreescu, L.A. Luck, Studies of the binding and signaling of surface-immobilized ..., Anal. Biochem. (2008), doi:10.1016/j.ab.2007.12.035

an average ζ-potential value of -29.1 ± 4.1 mV. In the presence of GGR–WT, the ζ-potential value was -19.3 ± 2.0 mV, suggesting a partial modification with the AuNPs. When the GGR–Cys was added, the particles were nearly neutral in charge (with a ζ-potential value of -4.25 ± 6.6 mV, indicating nearly complete coverage of the particles by a protein coating. The PSD of AuNPs in Tris buffer determined using the dynamic light scattering analyzer (Fig. 3A) indicates an average size of 42.5 nm. For the GGR–WT, the PSD shows an average diameter of 59.4 nm, whereas for the GGR–Cys, the average size of the aggregates formed was 139.6 nm.

These findings were also supported by the HR–TEM analysis. Fig. 4A shows the HR–TEM image of the bare AuNPs obtained by chemical precipitation of Au^{3+} with isoascorbic acid used for protein immobilization. As can be seen in the figure, the nanoparticles are quite uniform and monodispersed. The same behavior was observed when the GGR–WT protein was added to the solution. When GGR–Cys was used, the particles formed large aggregates (Fig. 3C). Analysis of a single AuNP + GGR–Cys at a lower magnification shows the presence of a thin layer on the surface of the particle. We speculate that this layer could be attributed to the protein, which is 35 Å wide and 65 Å long. The characteristics (ζ-potential, average particle size, UV–Vis peaks, and color) of the three configurations tested (AuNPs, AuNPs + GGR–WT, and AuNPs + GGR–Cys) are summarized in Table 1.

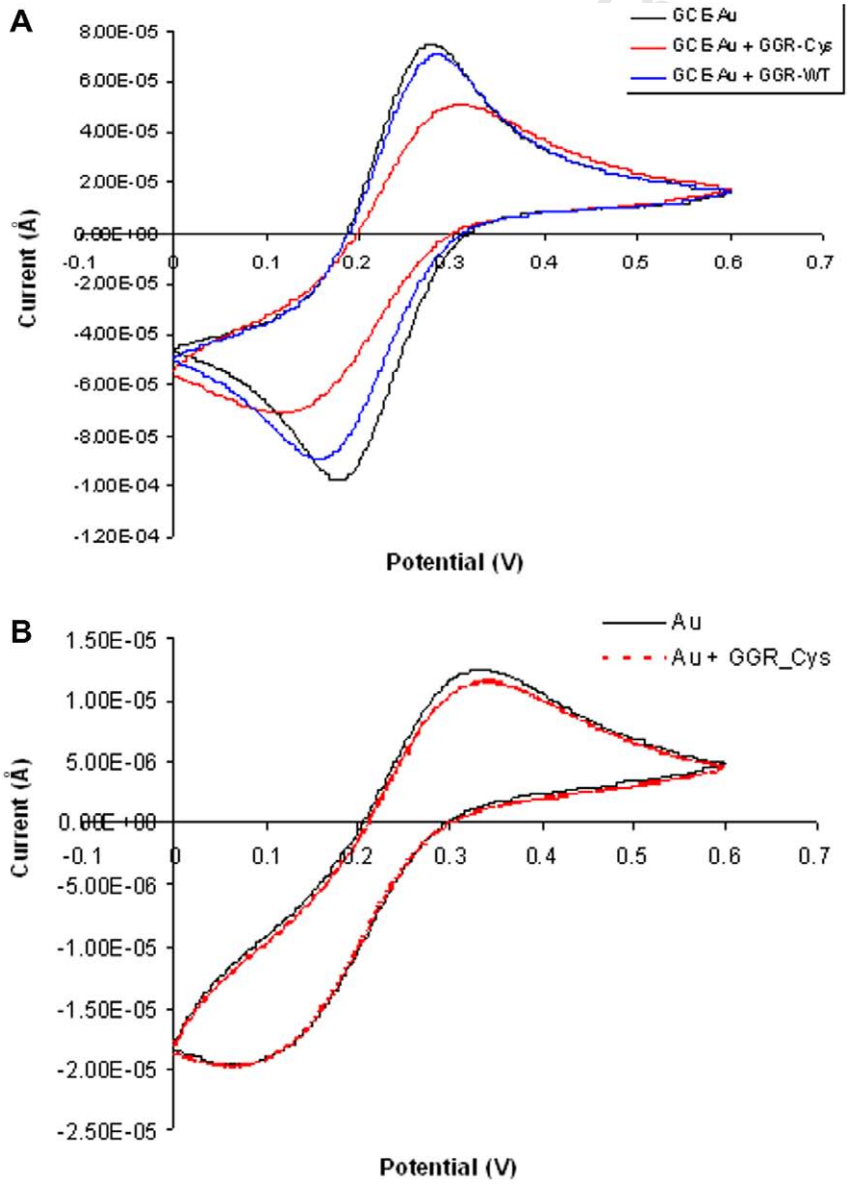

Fig. 6. (A) Cyclic voltammograms of GCE–AuNP electrode before and after modification with GGR–WT and GGR–Cys in 10 mM $K_3Fe(CN)_6$ as redox probe. (B) Cyclic voltammograms of a conventional gold electrode before and after modification with GGR–Cys. Scanning range: 0 to 0.6 V versus Ag/AgCl reference electrode at 50 mV/s.

Please cite this article in press as: S. Andreescu, L.A. Luck, Studies of the binding and signaling of surface-immobilized ..., Anal. Biochem. (2008), doi:10.1016/j.ab.2007.12.035

Fabrication of electrochemical biosensor for detection of glucose

The binding between the AuNPs and the two glucose receptor proteins was further investigated using CV after deposition of AuNPs on the surface of a working GCE. The recombinant proteins used in this work are engineered and act as an uptake system for a target ligand that in this case is glucose. The receptor binds D-glucose with a K_d of 0.1 μM. The binding of D-glucose produces a ligand-induced conformational change in the protein that is well characterized and has been used in a number of studies [15,17–19,23,26]. This specific binding, combined with the use of AuNPs for protein immobilization on an electrode surface, was employed in the current work in the construction of an electrochemical biosensor for the detection of glucose. A schematic of this experiment is illustrated in Fig. 5.

Biosensor fabrication

In our study, the AuNPs were electrodeposited on the GCE from a solution of $HAuCl_4$ according to a published literature procedure [28,29]. This resulted in a deposition of a smooth layer of aggregates of AuNPs that was confirmed by the change in the color of the working GCE surface from gray to yellow. The gold particles in the aggregate have an average size of approximately 50 nm, and this was also confirmed in our experiments by SEM (results not shown). This is in agreement with published literature data [28,29]. The modified GCE–AuNP electrode was further characterized by CV using $Fe^{II}(CN)_6^{4-}/Fe^{III}(CN)_6^{3-}$ as a model redox probe. Compared with the bare GCE, the peak potential separation ΔE_p was reduced from 93 to 70 mV for the GCE–AuNPs. Concurrently, a current amplification of both anodic and cathodic peaks was observed, suggesting that the presence of gold promoted the electron transfer at the surface of the electrode (results not shown).

We used this system first to investigate whether the binding of the protein on the GCE–AuNP surface follows the same trend as in the case of colloidal particles and then to check the stability of the binding for both the wild-type and Cys modified protein. For this purpose, the protein (GGR–WT or GGR–Cys) was immobilized on the GCE–AuNP surface. Immobilization was carried out by incubating the gold modified electrode for 1 h in a solution containing protein at a concentration of 7 μM. The electrode was washed several times to remove the excess of weakly bound proteins. CV using the $Fe^{II}(CN)_6^{4-}/Fe^{III}(CN)_6^{3-}$ model reversible electrochemical reaction was then employed to characterize the electron transfer properties on the surface of the electrode before and after protein binding. It is expected that the GGR–Cys will attach to the gold surface through its Cys residue. This will partially insulate the electrochemically active surface, hampering the electron transfer of the redox probe. Fig. 6 represents the cyclic voltammogram obtained from the GCE–AuNP electrode with GGR–WT or GGR–Cys and without protein. The cyclic voltammogram recorded after exposure to GGR–WT is nearly identical to that corresponding with the bare GCE–AuNP electrode. This implies that there is little or no change on the surface of the AuNPs, suggesting that the WT protein does not bind to the electrode surface. In contrast, the exposure of GGR–Cys to the AuNPs induced a significant decrease in the oxidation and reduction peaks in the CV spectrum, clearly indicating the deposition of a protein layer that partially insulates the electrode surface. To confirm the

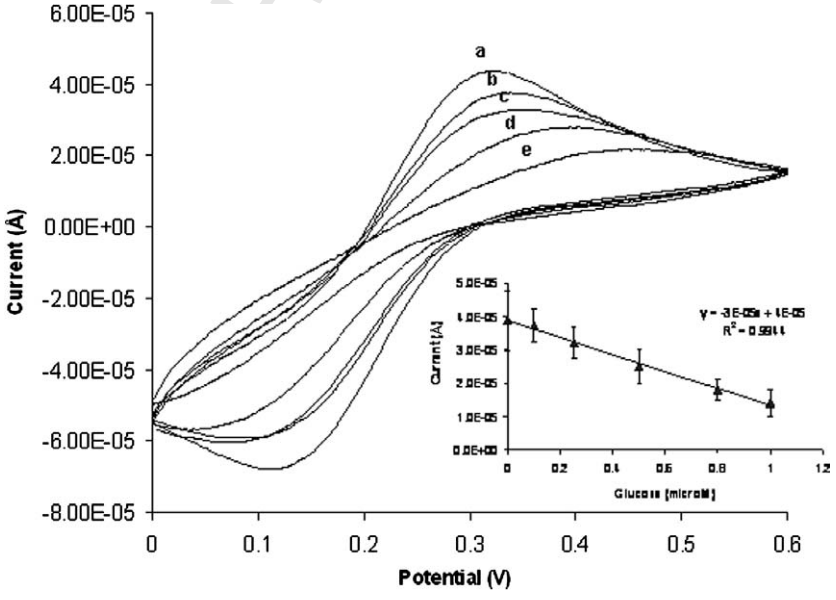

Fig. 7. Cyclic voltammograms of GCE–AuNP electrode modified with GGR–Cys after 5 min incubation with different glucose concentrations: 0 μM (a), 0.1 μM (b), 0.25 μM (c), 0.5 μM (d), and 1 μM (e). Cyclic voltammograms were recorded in 10 mM $K_3Fe(CN)_6$ as redox probe. Scanning range: 0 to 0.6 V versus Ag/AgCl reference electrode at 50 mV/s. Inset: Biosensor calibration curve for glucose. The error bars represent the standard deviation of triplicate measurements obtained with different electrodes.

Please cite this article in press as: S. Andreescu, L.A. Luck, Studies of the binding and signaling of surface-immobilized ..., Anal. Biochem. (2008), doi:10.1016/j.ab.2007.12.035

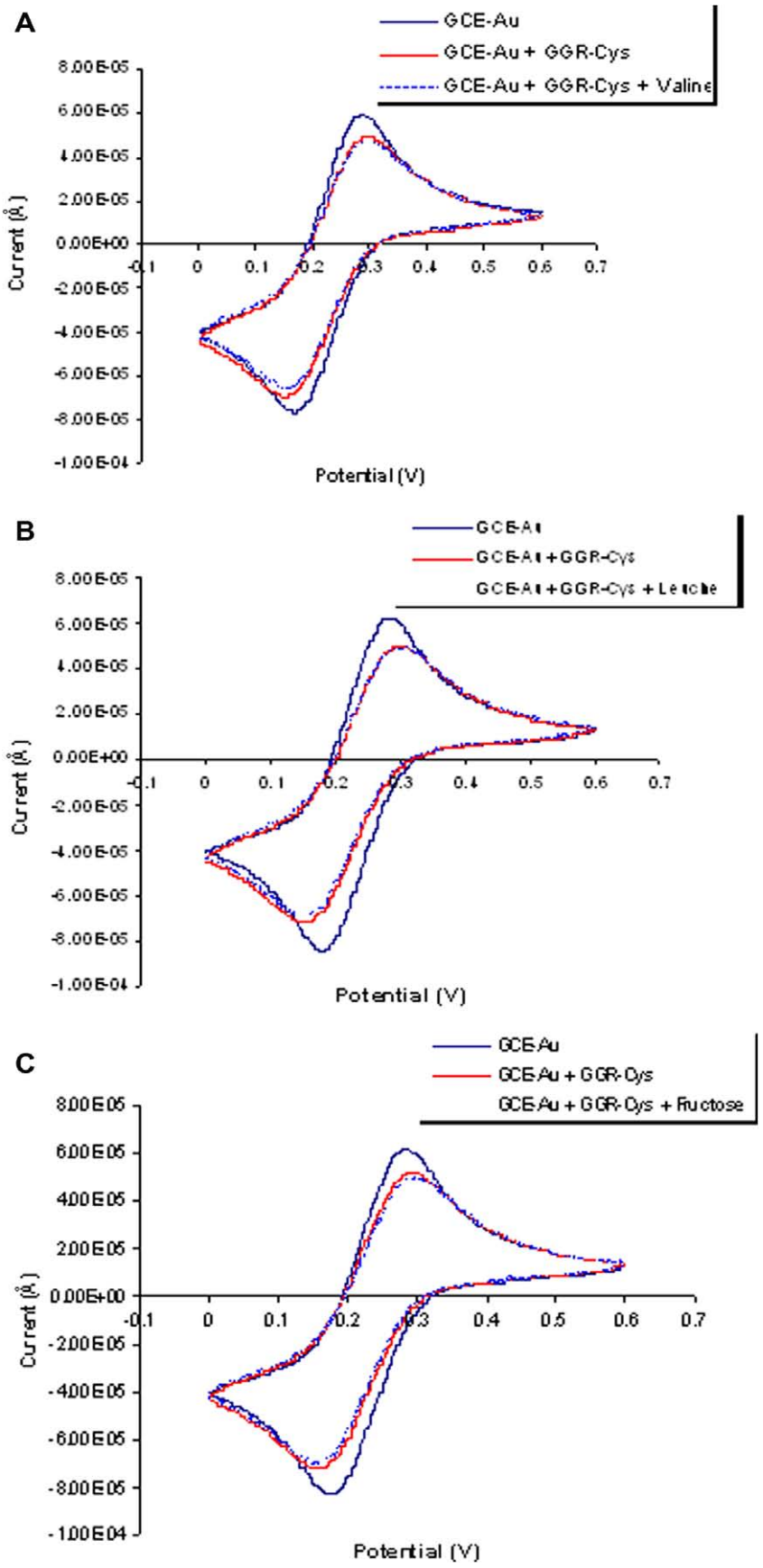

Fig. 8. Binding studies of the GCE–Au–GGR–Cys biosensor for valine (A), leucine (B), and fructose (C) in 10 mM $K_3Fe(CN)_6$ as redox probe. Scanning range: 0 to 0.6 V versus Ag/AgCl reference electrode at 50 mV/s.

Please cite this article in press as: S. Andreescu, L.A. Luck, Studies of the binding and signaling of surface-immobilized ..., Anal. Biochem. (2008), doi:10.1016/j.ab.2007.12.035

role of the AuNPs, for comparison purposes, we performed similar studies with a conventional gold electrode. In the same experimental conditions, the electrochemical response of the gold electrode was significantly reduced (1.25×10^{-5} Å) as compared with that of the GCE–AuNPs (7.8×10^{-5} Å). After incubation in a solution of GGR–Cys, the protein binds to the Au electrode, but the decrease in the signal was very small (Fig. 6B).

Detection of glucose

The GCE–AuNPs with GGR–Cys immobilized on the surface were used as a biosensor for the detection of glucose. This system is based on the specificity of the glucose receptor and the ligand-induced conformational change that occurs after glucose binds to the protein. Studies showed that when a ligand binds to a periplasmic binding protein, such as the GGR used in the current work, the protein undergoes a structural change [14]. In previous studies, this effect was studied extensively and confirmed by atomic force microscopy [22], quartz crystal microbalance [15–17,20], and electrochemical impedance spectroscopy [18,21]. It was demonstrated that the flexible ligand-free protein undergoes a conformational change to a more rigid structure after ligand binding [20]. In the current work, after immersion of the GGR–Cys modified electrode in a solution containing glucose, the cyclic voltammogram shows that the oxido/reduction current decreases concurrently with a shift toward more positive potentials shown in Fig. 7. This is a result of the glucose binding, associated with the closing structure of the protein around its binding pocket, hindering the electron transfer of the redox probe on the active surface of the electrode. These observations are in agreement with previous impedance spectroscopy studies that showed an increase in the electron transfer resistance after glucose binding [18,22]. Fig. 7 shows the cyclic voltammogram of the GCE–AuNP electrode modified with GGR–Cys before and after 5 min incubation with different concentrations of glucose ranging from 0.1 to 1 μM. The decrease in the current was proportional with the glucose concentration. No further decrease in the signal was obtained at concentrations higher than 1 μM. Increasing the incubation time (e.g., 1 h, 12 h) does not result in a lower detection limit, showing that glucose binding is a nearly immediate effect. The detection limit of the sensor was 0.18 μM, calculated based on the standard deviation and the slope, using the $3\sigma/S$ formula, where σ is the standard deviation of the responses of three blank samples obtained with different electrodes and S is the slope of the calibration curve.

Although in other previous studies we have shown that glucose does not bind to flat gold surfaces [15,17], we did control experiments to check for the possible binding of glucose to the AuNPs. Results showed that incubation of the bare GCE–AuNP electrode in a glucose solution has no effect on the electrochemical current, indicating that binding of the glucose with the immobilized GGR protein on the AuNPs is responsible for the observed decrease of the redox peaks.

When the GCE–AuNP–GGR–Cys electrode was incubated with three other compounds that do not bind GGR (β-D-fructose, L-valine, and L-leucine), no decrease in the electrochemical signal was observed (Fig. 8). These results show that the proposed biosensor specifically binds its target sugar and shows no response to compounds that are not natural ligands.

Conclusions

We have studied the surface chemistry and interactions of AuNPs with a wild-type and a genetically engineered thiol-containing glucose receptor protein, and we used this system to construct an electrochemical system for selective detection of glucose. The interaction of proteins with AuNPs and the surface chemistry was studied with UV–Vis spectroscopy, TEM, ζ-potential, and PSD analysis, and the results were confirmed with CV. The gold colloids form large aggregates in the presence of the thiol-containing protein. This is due to the strong binding between the gold and the SH of the cysteine group that was genetically engineered in the protein sequence. Under the same experimental conditions (pH, temperature, and buffer solution) but using the WT protein, gold colloids do not aggregate in the same manner. These experiments suggest that the surface-exposed cysteine is key to the binding of the protein to the AuNPs. The electrochemical GGR-based biosensor developed in this work is suitable for selective determination of glucose in the micromolar concentration range, with a detection limit of 0.25 μM. The AuNP reagentless glucose biosensor described here provides a unique addition to the currently available methods to detect glucose. As compared with classical solid gold electrodes, the use of AuNP modified GCE offers several advantages such as a large surface area that provides multiple binding points for proteins (thereby facilitating loading of more protein molecules), high conductivity, and increased sensitivity. The application of this strategy of combined genetic engineering, AuNPs, and electrochemistry serves as a useful tool for the study of receptor–ligand interactions.

Acknowledgments

This work was supported by NSF CTS 0329698 (L.A.L.), U.S. Army Breast Cancer Research Grant Concept Award W81XWH-06-1-0621 (L.A.L.), and U.S. Army W911WF-05-1-0339 (S.A.).

References

[1] C.A. Mirkin, R.L. Letsinger, R.C. Mucic, J.J. Storhoff, A DNA-based method for rationally assembling nanoparticles into macroscopic materials, Nature 382 (1996) 607–609.
[2] O.V. Salata, Applications of nanoparticles in biology and medicine, J. Nanobiotechnol. 2 (2004) 1–6.

[3] N.C. Tansil, Z.Q. Gao, Nanoparticles in biomolecular detection, Nano Today 1 (2006) 28–37.
[4] J.H. Kim, J.S. Kim, H. Choi, S.M. Lee, K.N. Yu, E. Kuk, Y.K. Kim, D.H. Jeong, M.H. Cho, Y.S. Lee, Nanoparticle probes with surface enhanced Raman spectroscopic tags for cellular cancer targeting, Anal. Chem. 78 (2006) 6967–6973.
[5] S. Mandal, S. Phadtare, M. Sastry, Interfacing biology with nanoparticles, Curr. Appl. Physics 5 (2005) 118–127.
[6] S.G. Penn, L. He, M.J. Natan, Nanoparticles for bioanalysis, Curr. Opin. Chem. Biol. 7 (2003) 609–615.
[7] J. Wang, Nanoparticle-based electrochemical bioassay of proteins, Electroanalysis 19 (2007) 769–776.
[8] S. Guo, E. Wang, Synthesis and electrochemical applications of gold nanoparticles, Anal. Chim. Acta 598 (2007) 181–192.
[9] P. Yanez-Sedeno, J.M. Pingarron, Gold nanoparticles-based electrochemical biosensors, Anal. Bioanal. Chem. 382 (2005) 884–886.
[10] I. Willner, R. Baron, B. Willner, Integrated nanoparticle–biomolecule systems for biosensing and bioelectronics, Biosens. Bioelectron. 22 (2007) 1841–1852.
[11] C. Lei, S-Q. Hu, N. Gao, G-L. Shen, R-Q. Yu, An amperometric hydrogen peroxide biosensor based on immobilizing horseradish peroxidase to a nano-Au monolayer supported by sol–gel derived carbon ceramic electrode, Bioelectrochemistry 65 (2004) 33–39.
[12] W. Yang, J. Wang, S. Zhao, Y. Sun, C. Sun, Glucose oxidase/colloidal gold nanoparticles immobilized in Nafion film on glassy carbon electrode: Direct electron transfer and electrocatalysis, Bioelectrochemistry 69 (2006) 158–163.
[13] Y. Hu, A. Das, M.H. Hecht, G. Scoles, Nanografting de novo proteins onto gold surfaces, Langmuir 21 (2005) 9103–9109.
[14] F.A. Quiocho, Atomic structures of perisplasmic binding proteins and the high affinity active transport systems in bacteria, Philos. Trans. R. Soc. Lond. 326 (1990) 341–351.
[15] K.S. Carmon, R.E. Baltus, L.A. Luck, A piezoelectric quartz crystal biosensor: The use of two single cysteine mutants of the periplasmic E. coli glucose/galactose receptor as target proteins for the detection of glucose, Biochemistry 43 (2004) 1429–1456.
[16] K.S. Carmon, R.E. Baltus, L.A. Luck, A biosensor for estrogenic substances using the quartz crystal microbalance, Anal. Biochem. 345 (2005) 277–283.
[17] L.A. Luck, M.J. Moravan, J.E. Garland, B. Salopek-Sondi, D. Roy, Chemisorptions of bacterial receptors for hydrophobic amino acids and sugars on gold for biosensor applications: A surface plasmon resonance study of genetically engineered proteins, Biosens. Bioelectron. 19 (2003) 249–259.
[18] J. Wang, K.S. Carmon, L.A. Luck, I.I. Suni, Electrochemical impedance biosensor for glucose detection utilizing a periplasmic E. coli receptor protein, Electrochem. Solid-State Lett. 8 (2005) H61–H64.
[19] A. Tripathi, J. Wang, L.A. Luck, I.I. Suni, Nanobiosensor design utilizing a periplasmic E. coli receptor protein immobilized within Au/polycarbonate nanopores, Anal. Chem. 79 (2007) 1266–1270.
[20] R.E. Baltus, K.S. Carmon, L.A. Luck, Quartz crystal microbalance with immobilized protein receptors: A comparison of response to ligand binding for direct protein immobilization and protein attachment via a disulfide linker, Langmuir 23 (2007) 3990–3995.
[21] J. Wang, L.A. Luck, I.I. Suni, Immobilization of the glucose–galactose receptor protein onto a Au electrode through a genetically engineered cysteine residue, Electrochem. Solid-State Lett. 10 (2007) 133–136.
[22] I. Sokolov, S. Venkatesh, L.A. Luck, Change in rigidity in the activated form of the glucose/galactose receptor from E. coli: A phenomenon that will be key to the development of biosensors, Biophys. J. 90 (2006) 1058–1063.
[23] R.M. de Lorimier, Y. Tian, H.W. Hellinga, Binding and signaling of surface-immobilized reagentless fluorescent biosensors derived from periplasmic binding proteins, Protein Sci. 15 (2006) 1936–1944.
[24] D. Andreescu, K.S. Tapan, D.V. Goia, Stabilizer free nanosize gold sols, J. Colloid Interface Sci. 298 (2006) 93–100.
[25] C.G. Blatchford, J.R. Campbell, J.A. Creighton, Plasma resonance-enhanced Raman scattering by absorbates on gold colloids: The effects of aggregation, Surf. Sci. 120 (1982) 435.
[26] S. Chah, M.R. Hammond, R.N. Zare, Gold nanoparticles as a colorimetric sensor for protein conformational changes, Chem. Biol. 12 (2005) 323–328.
[27] D. Aili, K. Enander, J. Rydberd, I. Lundstrom, L. Baltzer, B. Lieberg, Aggregation-induced folding of a de novo designed polypeptide immobilized on gold nanoparticles, J. Am. Chem. Soc. 128 (2006) 2194–2195.
[28] P. Yanez-Sedeno, J.M. Pingarron, Gold nanoparticles-based electrochemical biosensors, Anal. Bioanal. Chem. 382 (2005) 884–886.
[29] (a) V.C. Sanz, M.L. Mena, A. Gonzalez-Cortes, P. Yánez-Sedeno, J.M. Pingarron, Anal. Chim. Acta 528 (2005) 1; Q2
(b) M.L. Mena, P. Yánez-Sedeno, J.M. Pingarron, Anal. Biochem. 336 (2005) 20–26.

Quartz Crystal Microbalance (QCM) with Immobilized Protein Receptors: Comparison of Response to Ligand Binding for Direct Protein Immobilization and Protein Attachment via Disulfide Linker

Ruth E. Baltus,*,† Kendra S. Carmon,§,# and Linda A. Luck§,⊥

Department of Chemical and Biomolecular Engineering and Department of Chemistry and Biology, Clarkson University, Potsdam, New York 13699

Received September 27, 2006. In Final Form: January 17, 2007

Results from an investigation of the frequency response resulting from ligand binding for a genetically engineered hormone-binding domain of the α-estrogen receptor immobilized to a piezoelectric quartz crystal are reported. Two different approaches were used to attach a genetically altered receptor to the gold electrode on the quartz surface: (1) the mutant receptor containing a single solvent-exposed cysteine was directly attached to the crystal via a sulfur to gold covalent bond, forming a self-assembled protein monolayer, and (2) the N-terminal histidine-tagged end was utilized to attach the receptor via a 3,3-dithiobis[*N*-(5-amino-5-carboxypentyl)propionamide-*N*′,*N*′-diacetic acid] linker complexed with nickel. Previous studies have shown that these engineered constructs bind 17β-estradiol and are fully functional. Exposure of the receptor directly attached to the piezoelectric crystal to the known ligand 17β-estradiol resulted in a measurable frequency response, consistent with a change in conformation of the receptor with ligand binding. However, no response was observed when the receptor immobilized via the linker was exposed to the same ligand. The presence of the linker between the quartz surface and the protein receptor does not allow the crystal to sense the conformational change in the receptor that occurs with ligand binding. These results illustrate that the immobilization strategy used to bind the receptor to the sensor platform is key to eliciting an appropriate response from this biosensor. This study has important implications for the development of QCM-based sensors using protein receptors.

Introduction

There has been considerable interest in using quartz crystal microbalance (QCM) technology to examine adsorption phenomena at solid surfaces. This technique has been used in a variety of applications, primarily to monitor metallic deposition on surfaces. Recently the utilization of this technique for biological systems has come into vogue.[1,2] In the past decade, QCM-based sensors have been used to study kinetics of protein adsorption and antibody−antigen and protein−lipid membrane interactions where the mass change on the surface is quite large.[3−7] We have been interested in examining QCM response to smaller mass changes. Work in our laboratories has focused on using QCM to study interactions between protein receptors and small ligands.[8,9]

A QCM sensor utilizes an AT-cut piezoelectric quartz crystal film with gold electrodes deposited on both surfaces. Application of a radiofrequency voltage at the resonant frequency of the crystal excites the crystal into oscillation. Changes in mass, viscosity, conductivity, and stiffness of the layer near the crystal surface result in changes in the crystal frequency, which can be easily measured. When a rigid mass is added to the surface of the piezoelectric crystal, the resulting decrease in oscillation frequency can be quantitatively interpreted using the well-known Sauerbrey equation

$$\Delta f = -\frac{2f^2}{\sqrt{\rho_q \mu_q}}\Delta m = -C_f \Delta m \qquad (1)$$

where Δf is the frequency shift resulting from the additional mass per area, Δm, f is the intrinsic crystal frequency, ρ_q is the density of the quartz, and μ_q is the shear modulus of the quartz film.[10] For a 5 MHz crystal, $C_f = 56.5$ Hz cm^2/μg. When the added mass is not a rigid solid, as with many biological samples, the frequency response is dampened, resulting in a frequency shift that is less than predicted using eq 1. Recent papers have

* Corresponding author [e-mail baltus@clarkson.edu; telephone (315) 268-2368; fax (315) 268-6654].

† Departmet of Chemical and Biomolecular Engineering.

§ Department of Chemistry and Biology.

Present address: Department of Integrative Biology and Pharmacology, UT Houston Health Science Center, Houston, TX 77030.

⊥ Present address: Department of Chemistry, SUNY Plattsburgh, Plattsburgh, NY 12901.

(1) Marx, K. Quartz Crystal Microbalance: A Useful Tool for Studying Thin Polymer Films and Complex Biomolecular Systems at the Solution-Surface Interface. *Biomacromolecules* **2003**, *4*, 1099−1120.

(2) Janshoff, A.; Galla, H. J.; Steinam, C. Piezoelectric Mass-Sensing Devices as Biosensors−An Alternative to Optical Biosensors? *Angew. Chem.* **2000**, *39*, 4004−4032.

(3) Hook, F.; Kasemo, B. Variations in Coupled Water, Viscoelastic Properties, and Film Thickness of a Mefp-1 Protein Film during Adsorption and Cross-linking: A Quartz Crystal Microbalance with Dissipation Monitoring, Ellipsometry, and Surface Plasmon Resonance Study. *Anal. Chem.* **2001**, *73*, 5796−5804.

(4) Hook, F.; Rodahl, M.; Kasemo, B.; Brzezinski, P. Structural changes in hemoglobin during adsorption to solid surfaces: Effects of pH, ionic strength, and ligand binding. *Proc. Natl. Acad. Sci. U.S.A.* **1998**, *95*, 12271−12276.

(5) Caruso, F.; Furlong, D. N.; Niikura, K.; Okahata, Y. In-situ measurement of DNA immobilization and hybridization using a 27 MHZ quartz crystal microbalance. *Colloids Suf. B: Biointerfaces* **1998**, *10*, 199−204.

(6) Decker, J.; Weinberger, K.; Prohaska, E.; Hauck, S.; Koblinger, C.; Wolf, H.; Hengerer, A. Characterization of a human pancreatic secretory trypsin inhibitor mutant binding to *Legionella pneumophila* as determined by a quartz crystal microbalance. *J. Immunol. Methods* **2000**, *233*, 159−165.

(7) Babacan, S.; Pivarnik, P.; Letcher, S.; Rand, A. G. Evalution of antibody immobilization methods for piezoelectric biosensor application. *Biosens. Bioelectron.* **2000**, *15*, 615−621.

(8) Carmon, K. S.; Baltus, R. E.; Luck, L. A. A Piezoelectric Quartz Crystal Biosensor: The Use of Two Single Cysteine Mutants of the Periplasmic *E. coli* Glucose/Galactose Receptor as Target Proteins for the Detection of Glucose. *Biochemistry* **2004**, *43*, 1429−1456.

(9) Carmon, K. S.; Baltus, R. E.; Luck, L. A. A Biosensor for Estrogenic Substances Using the Quartz Crystal Microbalance. *Anal Biochem.* **2005**, *345*, 277−283.

(10) Sauerbrey, G. *Z. Phys* **1959**, *155*, 206−222.

10.1021/la0628468 CCC: $37.00
Published on Web 02/27/2007

addressed this deviation from the Sauerbrey equation with efforts to account for the viscoelastic properties of the film on the surface.[3,4,11] This expands the versatility of the QCM methodology and enables application of the technology to biological systems.

In recent years, work in our laboratories has focused on experimental studies of receptor−ligand interactions using QCM with immobilized genetically engineered protein receptors. A QCM study of glucose binding to a mutant-immobilized glucose/galactose receptor from *Escherichia coli* was undertaken.[8] Results showed a frequency response to glucose binding that was significantly larger than predicted by considering only the mass contribution from glucose. We attributed this unexpectedly large response to ligand-induced conformational changes in the protein.[8,12] When a ligand binds, the glucose/galactose-binding protein undergoes a structural change, as do many other periplasmic binding proteins.[13] The ligand-free protein is flexible and poised to capture the ligand. With ligand binding, the protein adopts a denser and more rigid form that enables the transport of ligand to the transport or chemotaxis assemblies in the membrane. The sensitivity of the QCM to the characteristics of the film in the vicinity of the crystal surface enables the QCM to sense receptor binding to this small ligand. Calculations of the frequency shift expected when a flexible, viscous film is replaced by a thinner, denser, and more rigid film were consistent with this interpretation. An examination of the rigidity of this immobilized glucose receptor with and without ligand using atomic force microscopy provided additional support for this interpretation.[14]

A similar investigation was undertaken to examine the response of a QCM biosensor that utilizes a genetically engineered histidine-tagged construct of the hormone-binding domain of the estrogen receptor containing amino acids 304−554 to various estrogenic substances.[9] In this construct, the two naturally occurring cysteine residues on amino acids 381 and 530 were changed to serine residues, leaving only one solvent-exposed cysteine residue at position 417 for binding to the gold electrode. Exposure of the immobilized estrogen receptor to various estrogenic substances (i.e, 17β-estradiol, tamoxifen, diethylstilbestrol) yielded frequency shifts considerably larger than expected from mass considerations alone. Again, it is proposed that the QCM is sensing ligand-induced conformational changes when this receptor binds to ligand. Our results also indicate that the frequency response of the immobilized estrogen receptor is dependent upon the type of estrogen mimic, antagonist or agonist. These observations are believed to result from different conformational changes induced by the different ligands.

The objective of the current study was to examine the effect of immobilization strategy on the QCM frequency response to ligand binding experienced by the estrogen receptor. The thiol linker 3,3-dithiobis[*N*-(5-amino-5-carboxypentyl)propionamide-*N*′,*N*′-diacetic acid] complexed with nickel (Ni-NTA) was used as a means to immobilize the genetically engineered ligand-binding domain of the estrogen receptor. The thio end of the linker binds to the gold surface via a gold−sulfur bond and provides a self-assembled monolayer on the gold. The Ni-NTA chelate end, which is commonly used for histidine-tagged protein purification or separation, binds to the genetically engineered binding domain of the estrogen receptor. In this paper, the frequency response to 17β-estradiol is compared for the receptor directly immobilized on the gold surface to receptor immobilized via a Ni-NTA linker.

Experimental Section

Estrogen Receptor Protein Production for Experiments. The protein used in this study was expressed from a pet-15b construct of the ligand-binding domain of the α-estrogen receptor encompassing residues 304−554 transformed into BL21(DE3) pLysS cells with cysteine to serine mutations at positions 381 and 530 ($_{dm}$HBD-ER). The His-tagged $_{dm}$HBD-ERs were purified according to standard protocols described in previous publications.[15] This double mutant was used for all experiments reported here and is the same receptor that was used in our earlier reported study.[9] For brevity, we will simply use $_{dm}$HBD-ER when referring to this protein. The mutant receptor, with and without the His-tag, binds estradiol and xenoestrogens with wild-type affinity.[9,15]

QCM Sensor. The Research Quartz Crystal Microbalance (RQCM) from Maxtek, Inc., is composed of the sensor, oscillator unit, frequency counter, voltage supply, and PC interface connection for signal output visualization. The RQCM sensors employed were commercially available 5 MHz polished AT-cut quartz crystals (2.54 cm diameter) with gold electrodes (1.27 cm diameter) on both sides. The crystal was placed in the holder and positioned by an O-ring so that only one side was exposed to the protein, ligand, and buffer solutions. A 250 mL beaker containing 200 mL of 50 mM Tris, 10% glycerol, and 10 mM β-mercaptoethanol (pH 8.0) (T/G buffer) served as the "measurement cell". A small plastic ring, which was part of the crystal holder, formed a small well above the electrode surface. Protein and ligand solutions were incubated on the crystal surface in this well. The experimental system is described in detail elsewhere.[8]

Self-Assembled Protein Monolayer. *Direct Attachment of $_{dm}$HBD-ER to the Gold Electrode Surface.* The frequency of the clean quartz crystal was measured initially by immersing the crystal holder in the QCM measurement cell with T/G buffer. After a stable baseline had been recorded, the holder was removed from the measurement cell, and 400 μL of 1 mg/mL $_{dm}$HBD-ER was incubated on the crystal surface. An incubation time of 1 h was used to ensure maximum protein attachment. After incubation, the crystal with immobilized protein was washed and returned to the measurement cell. Frequency was monitored until a stable reading was again obtained.

Exposure of the Self-Assembled Protein Monolayer to 17β-Estradiol. The crystal with immobilized $_{dm}$HBD-ER was then incubated with 400 μL of 20 μM 17β-estradiol. Because 17β-estradiol is insoluble in water, an ethanol in water solution was used, with ethanol concentration of <1%. After 30 min, the estradiol solution was rinsed off the crystal and the crystal was immersed in the frequency measurement cell. When a stable frequency value was achieved, the crystal was removed from the measurement cell.

Receptor Immobilization via Ni-NTA Linker. The sequence of experiments carried out with the Ni-NTA linker is depicted in Figure 1.

Immobilization of Ni-NTA Linker. Initially, the frequency of a clean crystal was measured by immersing the crystal holder into the QCM measurement cell. After a stable baseline had been recorded, the crystal holder was removed from the measurement cell and incubated for 30 min at room temperature with 100 μM 3,3-dithiobis-[*N*-(5-amino-5-carboxypentyl)propionamide-*N*′,*N*′-diacetic acid] (NTA) purchased from DOJINDO (Kumamoto, Japan) followed by washing with distilled water. The quartz crystal was then immersed in 0.1 M $NiSO_4$ for 30 min. After solution was rinsed off the crystal, the frequency of the crystal was again measured by re-immersing

(11) Hunt, W.; Stubbs, D.; Lee, S. Time-dependent Signature of Acoustic Wave Biosensors. *IEEE* **2003**, 890−901.

(12) Luck, L. A.; Falke, J. J. ^{19}F NMR Studies of the D-Galactose Chemosensory Receptor. 1. Sugar Binding Yields a Global Structural Change. *Biochemistry* **1991**, *30*, 4248−4256.

(13) Quiocho, F. A. Atomic Structures of Periplasmic Binding Proteins and the High Affinity Active Transport Systems in Bacteria. *Philos. Trans. R. Soc. London* **1990**, *326*, 341−351.

(14) Sokolov, I.; Venkatesh, S.; Luck, L. A. Change in Rigidity in the Activated Form of the Glucose/Galactose Receptor from *E. coli*: A Phenomenon That Will Be Key to the Development of Biosensors. *Biophys. J.* **2006**, *90*, 1058−1063.

(15) Tamrazi, A.; Carlson, K. E.; Daniels, J. R.; Hurth, K. M.; Katzenellenbogen, J. A. Estrogen Receptor Dimerization: Ligand Binding Regulates Dimer Affinity and Dimer Dissociation Rate. *Mol. Endocrinol.* **2002**, *16*, 2706−2719.

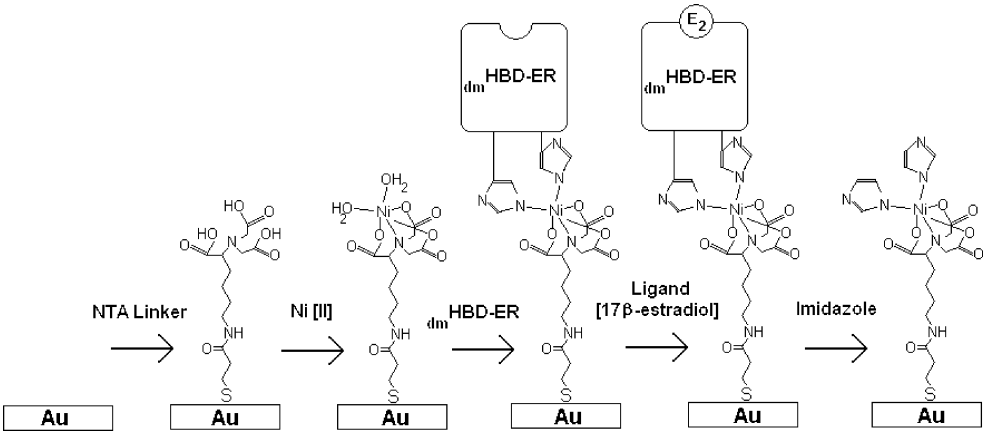

Figure 1. Schematic diagram of the steps involved in attachment of $_{dm}$HBD-ER to the gold electrode, followed by exposure to 17β-estradiol and imidazole.

the crystal holder in the QCM measurement cell containing T/G buffer. The Ni-NTA linker is attached to the gold electrode by a sulfur−gold bond, as shown in Figure 1.

Attachment of $_{dm}$HBD-ER to the Ni-NTA Linker. The crystal with attached Ni-NTA linker was removed from the QCM measurement cell and incubated with 400 μL of a 1.0 mg/mL solution of $_{dm}$-HBD-ER in T/G buffer for 1 h. The crystal surface was again rinsed and returned to the QCM measurement cell with T/G buffer. The frequency was again recorded once a stable value was observed. The histidine tag on the $_{dm}$HBD-ER binds to the nickel that is complexed with the NTA linker, as shown in Figure 1.

Exposure to 17β-Estradiol. The crystal holder was again removed from the measurement cell, and a 400 μL quantity of 17β-estradiol in ethanol solution (<1% ethanol in water) was introduced to the crystal surface. Experiments were conducted with solutions with estradiol concentrations of 2 and 20 μM. At 30 min intervals, the crystal was rinsed and immersed in the QCM measurement cell with T/G buffer and frequency was measured. A 2 h incubation time was found to be sufficient for complete ligand binding.

Exposure to Imidazole. To verify the QCM frequency response to the addition of $_{dm}$HBD-ER, the crystal with immobilized $_{dm}$HBD-ER was incubated with imidazole solution for 1 h. Imidazole will compete for the NTA sites with the histidine residues of the protein, resulting in protein removal, as shown in the last step in Figure 1. The effect of imidazole was examined for ligand-free immobilized $_{dm}$HBD-ER as well as for immobilized $_{dm}$HBD-ER that had been exposed to 17β-estradiol. Experiments were conducted with solutions with imidazole concentrations of 0.5 and 1.0 M. Following incubation with imidazole, the crystal holder was again immersed in the QCM measurement cell with T/G buffer for frequency measurements.

Results and Discussion

$_{dm}$HBD-ER. To produce sufficient quantities of protein for this study, a construct of the ligand-binding domain of the estrogen receptor that could be expressed in bacterial cells was used. In the wild-type protein, three cysteines are solvent exposed and can form interdomain disulfide bonds, leading to protein aggregation and denaturation. The double cysteine to serine mutant was created to circumvent these problems. Also, this double cysteine to serine mutant provided a single solvent-exposed cysteine residue, which was utilized to immobilize the receptor directly on the gold surface of the quartz crystal microbalance. There is one buried cysteine residue (447) that was left intact.

The six histidines at the N terminus of the protein served a dual purpose for this study. First, the N-terminal histidine tag is used to purify the protein via a nickel−nitrilotriacetic acid (NTA) resin. Second, this His-tag was used to immobilize the receptor to the NTA self-assembled monolayer on the gold electrode surface, as shown in Figure 1.

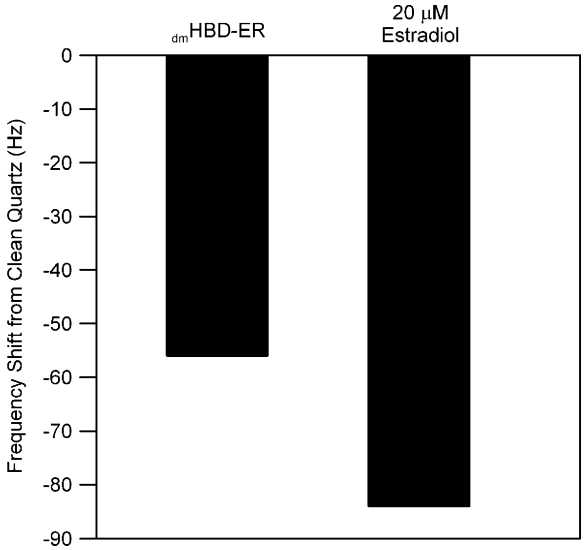

Figure 2. QCM response to direct attachment of $_{dm}$HBD-ER, followed by exposure to estradiol. The standard deviation in each frequency measurements is ±1 Hz.

Direct Attachment of $_{dm}$HBD-ER to the Gold Electrode Surface. The results from QCM frequency measurements for direct attachment of $_{dm}$HBD-ER to the gold electrode surface followed by exposure to estradiol are shown in Figure 2. These results have been reported previously.[9] Immobilization of $_{dm}$-HBD-ER to the crystal surface resulted in a decrease in crystal frequency of 54 Hz. Crystallography measurements have shown that HBD-ER with bound estradiol is a dimer with dimensions of approximately 55 Å × 55 Å × 64 Å, as shown in Figure 3.[16] Given the position of C417, it is expected that the $_{dm}$HBD-ER dimer will occupy a footprint of approximately 55 Å × 55 Å (3025 Å^2). Using the Sauerbrey equation (eq 1) with the molecular mass of HDB-ER (62 kDa), a frequency response of 16 Hz is predicted for monolayer coverage of this receptor. This predicted value is ~3−4 times smaller than the measured frequency shift.

The Sauerbrey equation is derived for a rigid film added to the piezoelectric surface. The protein film is expected to be reasonably fluid and viscous. This should lead to a dampening of the crystal oscillation, yielding an observed frequency shift that is smaller than the Sauerbrey prediction, not larger. There are a number of possible explanations for the larger than expected

(16) Brzozowski, A. M.; Pike, A. C. W.; Dauter, Z. E.; H. R.; Bonn, T.; Engstrom, O.; Ohman, L.; Greene, G. L.; Gustafsson, J.; Carlquist, M. Molecular Basis of Angonism and Antagonism in the Oestrogen Receptor. *Nature* **1997**, *389*, 753−758.

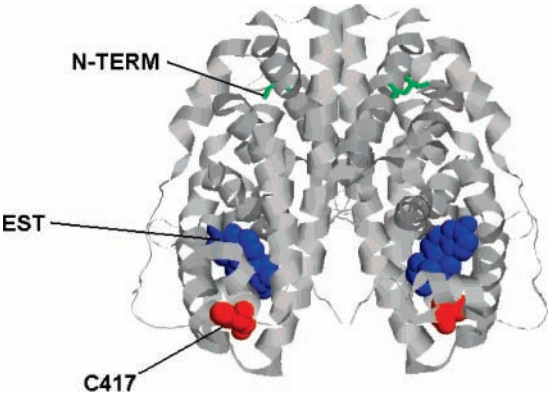

Figure 3. Representation of $_{dm}$HBD-ER dimer structure, from PDB file 1ERE.[16] EST is 17β-estradiol, and N-TERM is the N-terminal end of the protein where the His-tag is located.

observed frequency shifts with receptor attachment. The gold surface has some roughness, as revealed by atomic force microscopy imaging. Therefore, the surface area available for protein attachment is larger by perhaps 20% than the area based on the surface coverage of the electrode.[17] It is also possible that multiple layers of receptor attach to the gold surface because of different orientations of the $_{dm}$HBD-ER monomers relative to each other. For example, one monomer could bind to the electrode via a sulfur to gold bond with C417. A dimer could then form with this monomer. If the C417 residue of the second monomer does not bind to the electrode, this residue is available to form a disulfide bond with C417 of a third monomer. As discussed in our earlier paper,[9] the effective size of the immobilized protein in a liquid environment is expected to be smaller than the size estimated from crystallography measurements. It is also possible that the $_{dm}$HBD-ER can immobilize at an orientation such that its footprint is smaller than that estimated from the dimensions illustrated in Figure 3.

The relatively large measured frequency shift may also be attributed to the hydration shell surrounding the immobilized protein, yielding a film with mass greater than expected from protein geometry. In a study of protein adsorption using ellipsometry, optical waveguide lightmode spectroscopy, and a quartz crystal microbalance, Hook et al.[3] found that the mass of adsorbed protein measured using QCM was 2−3 times larger than the mass determined using the optical techniques and 1.1−2 times larger than the mass predicted from protein geometry. They attributed the large mass determined by QCM to bound or coupled water, which is not sensed by the optical techniques.

Given the uncertainty in the estimation of the footprint occupied by immobilized $_{dm}$HBD-ER and in the interpretation of frequency measurements in terms of added mass, the difference between the Sauerbrey prediction and the observed frequency response is not unreasonable. It is also important to note that the uncertainty in our estimation of the amount of immobilized protein is not critical in our interpretation of frequency shifts resulting from ligand binding.

When $_{dm}$HBD-ER was exposed to 20 μM estradiol, an additional frequency shift of ~25 Hz was observed. Significant frequency shifts were also observed when HBD-ER was exposed to other ligands that are known to bind to the estrogen receptor.[16] All of the tested ligands are relatively small. Assuming that each receptor binds one molecule of estradiol (or each dimer binds two molecules of estradiol), we can estimate the frequency shift expected from ligand binding on the surface. With an estradiol

(17) Sokolov, I. Personal communication, data not shown.

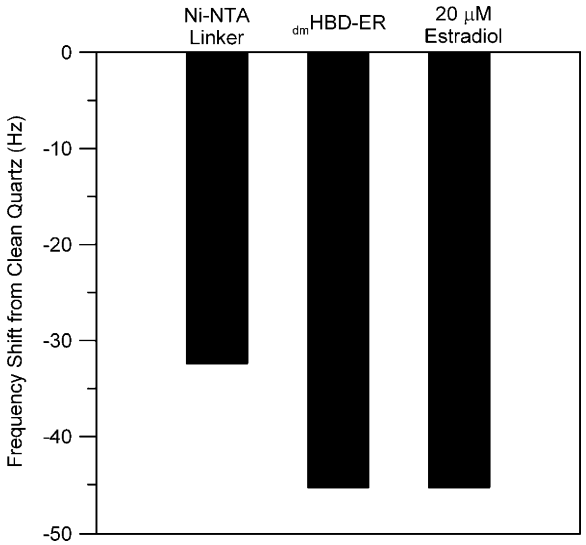

Figure 4. QCM response to attachment of Ni-NTA linker and immobilization of $_{dm}$HBD-ER, followed by exposure to estradiol. The standard deviation in each frequency measurements is ±1 Hz.

molecular mass of 272.38 g/mol, the Sauerbrey equation (eq 1) predicts a frequency shift of <1 Hz with the addition of this small mass to the surface. A similar unexpectedly large frequency response was also observed in similar experiments in our laboratory that involved glucose binding to a genetically engineered glucose/galactose receptor that was attached via a cysteine residue to the quartz film.[8] We attributed the large frequency response to ligand-induced conformational changes in the protein that are sensed by the QCM. These observations are consistent with calculations of the frequency response based on a viscoelastic model of the protein film where the protein undergoes a change in conformation from a flexible and viscous ligand-free protein film to a more rigid film upon ligand binding. This explanation is also consistent with atomic force microscopy studies showing an increase in the Youngs modulus of the glucose receptor film with ligand binding.[14] We speculate that the $_{dm}$HBD-ER undergoes similar ligand-induced structural changes that are sensed by the QCM.

$_{dm}$HBD-ER with Ni-NTA Linker. Results from QCM frequency measurements tracking the crystal response to immobilization of Ni-NTA linker to the gold electrode surface, attachment of $_{dm}$HBD-ER to the linker, and exposure to estradiol and/or imidazole are shown in Figures 4−6.

In each experiment involving the Ni-NTA linker, the frequency of the quartz crystal decreased by 30−50 Hz with immobilization of the NTA followed by complexation with Ni. The Sauerbrey equation (eq 1) was used to estimate the frequency response expected for this linker. As shown in Figure 1, the linker attaches to the gold surface via a sulfur−gold bond. Therefore, the area occupied by linker on the surface can be estimated using the van der Waals radius for sulfur (0.185 nm), giving an estimated coverage area of 0.108 nm^2 per linker molecule. With a molecular mass for the Ni-NTA complex of 444 g/mol, calculations using the Sauerbrey equation yield an expected frequency decrease of 39 Hz if the gold electrode surface is saturated with a monolayer of the Ni-NTA linker complex. The experimentally observed frequency response values are in reasonable agreement with this prediction, indicating that this picture of the surface coverage is accurate. These results indicate that the Ni-NTA on the surface is closely packed, providing for a reasonably rigid SAM film.

Upon attachment of $_{dm}$HBD-ER to the immobilized linker, the frequency of the piezoelectric crystals decreased an additional

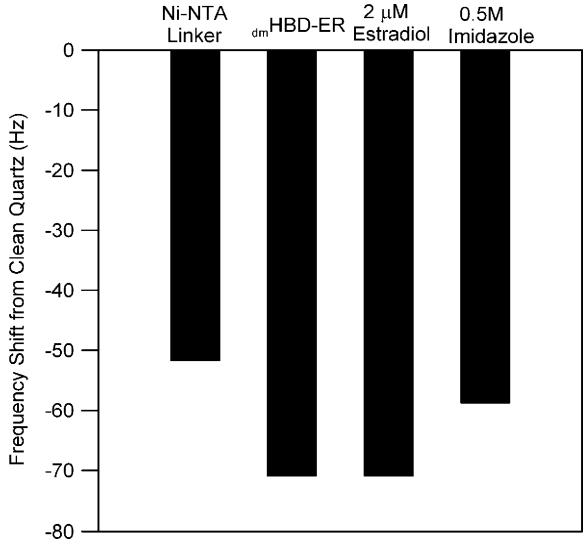

Figure 5. QCM response to attachment of Ni-NTA linker, $_{dm}$HBD-ER immobilization, and exposure to estradiol, followed by exposure to imidazole. The standard deviation in each frequency measurements is ±1 Hz.

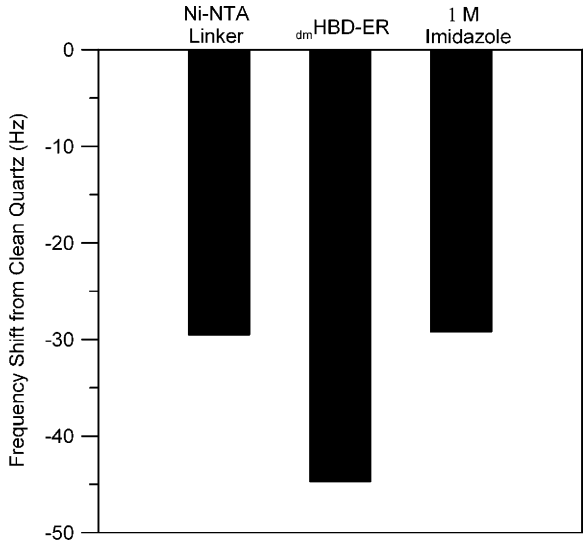

Figure 6. QCM response to attachment of Ni-NTA linker and immobilization of $_{dm}$HBD-ER, followed by exposure to imidazole. The standard deviation in each frequency measurements is ±1 Hz.

13−19 Hz. Given the receptor dimensions as estimated from crystallography and the position of the N-terminal end of the HBD-ER, it is expected that the dimer will occupy a footprint ranging from 55 Å × 55 Å (3025 Å^2) to 55 Å × 64 Å (3520 Å^2). With a dimer molecular weight of 62000 Da and this range of surface coverage, the Sauerbrey equation predicts a frequency shift of 16−19 Hz if the $_{dm}$HBD-ER behaves as a rigid solid on the surface, in agreement with our observations. This comparison of our experimental observations to the Sauerbrey prediction indicates that the linker with attached receptor is a reasonably rigid complex on the gold surface.

The frequency shift in response to receptor immobilization for protein directly attached to the gold electrode is 3−4 times larger than the response observed when the receptor is attached via the Ni-NTA linker. As discussed earlier in this paper, it is likely that some surface roughness is providing an increase in the area for immobilization for protein that is directly attached to the gold surface. However, a considerably smoother surface is expected once the gold is coated with a SAM of Ni-NTA. Therefore, some of this difference in frequency response can be attributed to differences in the effective area for immobilization. It is also likely that the His-tag on the end of the receptor allows some flexibility of the protein−linker complex when it is attached to the NTA monolayer, discouraging close binding of adjacent receptors. Therefore, it is possible that the protein is more compact when attached directly to gold than when it is attached to Ni-NTA linker.

Exposure of the immobilized $_{dm}$HBD-ER to 2 and 20 μM estradiol yielded no change in frequency, as shown in the results presented in Figures 4 and 5. Assuming that each receptor binds one molecule of estradiol (or each dimer binds two molecules of estradiol), a very small (<1 Hz) frequency shift is again predicted for ligand binding. The Maxtek QCM is not sufficiently sensitive to detect this small change in frequency. Our observations are again consistent with the Sauerbrey prediction. Given estimates of the surface coverage of the $_{dm}$HBD-ER (discussed above) and assuming that each receptor binds one molecule of estradiol, 400 μL of ∼0.03 μM estradiol solution should provide sufficient estradiol to saturate the immobilized receptor. This concentration value is an order of magnitude smaller than the lowest concentration used for our measurements. Although no frequency response to estradiol was observed, we believe that estradiol is indeed binding to the bound HBD-ER, on the basis of observations reported by others. A previous study of estrogenic compounds using NTA immobilized receptor similar to our construct showed full binding capacity to estradiol, estone, estriol, and a number of xenoestrogens.[18] At the high concentration of estradiol used in our experiments, we are confident that the immobilized receptor is fully saturated with ligand.

The intriguing result from this study is that when $_{dm}$HBD-ER is attached to the QCM quartz film via a Ni-NTA linker, the QCM cannot sense ligand binding, whereas a large frequency response to ligand binding is observed when the $_{dm}$HBD-ER is directly attached to the quartz film, forming a self-assembled protein monolayer. We believe that the linker provides a sufficient "buffer" between the protein and the electrode surface that prohibits the quartz film from sensing the ligand-induced structural changes in the receptor.

Effect of Imidazole. Imidazole competes for coordination sites on the nickel ion of the Ni-NTA linker and thus can be used to remove bound protein from the linker. In Figure 5, results are presented for the change in frequency observed when bound $_{dm}$HBD-ER with attached estradiol was exposed to 0.5 M imidazole. Results for the change in frequency observed when bound $_{dm}$HBD-ER without attached ligand was exposed to 1 M imidazole are presented in Figure 6. In all cases, frequency increased following exposure of the receptor to imidazole, observations that are consistent with removal of mass from the surface, and it is likely that it is protein that is being removed. The results shown in Figure 5 show that following exposure to imidazole, the frequency "recovered" ∼65% of the decrease observed with $_{dm}$HBD-ER attachment. The results shown in Figure 6 show that frequency returned completely to the value measured prior to $_{dm}$HBD-ER attachment. These results support our conclusion that the frequency shift observed with exposure to the receptor results from protein attachment to the linker and not to some other phenomena occurring at the quartz surface.

It is not clear why exposure to 0.5 M imidazole did not result in complete frequency recovery when exposure to 1 M imidazole

(18) Pillon, A.; Boussioux, A.; Escande, A.; Ait-Aissa, S.; Gomez, E.; Fenet, H.; Ruff, M.; Moras, D.; Vignon, F.; Duchesne, M.; Casellas, C.; Nicolas, J. Binding Estrogenic Compounds to Recombinant Estrogen Receptor-alpha: Application to Environmental Analysis. *Environ. Health Perspect.* **2005**, *113*, 278−284.

appears to trigger complete protein removal. A 0.5 M solution should be more than sufficient imidazole to trigger removal of all of the attached protein. It may be that the ligand induced structural changes in receptor resulting from ligand binding reduces the susceptibility of the NTA chelation site to imidazole. Additional studies with imidazole appear to be warranted.

Conclusions

In this study, the effect of the strategy used to immobilize receptor protein to a piezoelectric quartz crystal surface has been examined. Detection of 17β-estradiol using a genetically engineered hormone-binding domain of the α-estrogen receptor was investigated. When the genetically engineered receptor is directly attached to the surface in a known orientation, a measurable and significant frequency response is observed with ligand binding. This response is believed to arise from conformational changes in the receptor in response to ligand binding. When receptor is attached to the quartz crystal via binding of the histidine-tagged N-terminal end to a linker covalently attached to the surface, no response to ligand binding is observed. With linker between the piezoelectric surface and the receptor protein, QCM cannot sense the conformational changes that result with ligand binding. Hence, small ligands cannot be detected when this strategy is used to attach receptor. This study emphasizes the importance of the immobilization method when using receptor proteins as the sensor platform with QCM. With direct attachment of the receptor creating a self-assembled protein monolayer, QCM can detect ligands that are too small to be detected from a mass basis alone.

Acknowledgment. We gratefully acknowledge funding for this work from the NIH (Grant R03-CA 89705), NSF Grant CTS-0329698, and U.S. Army Breast Cancer Research Grant Concept Award W81XWH-06-1-0621. We thank Dr. John Katzellenebogen for the plasmid HBD (residues 304−554) and many helpful discussions.

LA0628468

BIOCHEMISTRY AND MOLECULAR BIOLOGY EDUCATION
Vol. 35, No. 4, pp. 238–243, 2007

Articles

Molecular Modeling of Estrogen Receptor Using Molecular Operating Environment

Received for publication, March 29, 2006, and in revised form, January 19, 2007

Urmi Roy‡ and Linda A. Luck§¶

From the ‡Center for Advanced Materials Processing, Clarkson University, Potsdam, New York 13699-5665 and §Department of Chemistry, State University of New York, Plattsburgh, New York 12901

Molecular modeling is pervasive in the pharmaceutical industry that employs many of our students from Biology, Chemistry and the interdisciplinary majors. To expose our students to this important aspect of their education we have incorporated a set of tutorials in our Biochemistry class. The present article describes one of our tutorials where undergraduates use modeling experiments to explore the structure of an estrogen receptor. We have employed the Molecular Operating Environment, a powerful molecular visualization software, which can be implemented on a variety of operating platforms. This tutorial reinforces the concepts of ligand binding, hydrophobicity, hydrogen bonding, and the properties of side chains and secondary structure taught in a general biochemistry class utilizing a protein that has importance in human biology.

Keywords: Computational biology, biotechnology education, computers in research and teaching, molecular modeling, estrogen receptor, estradiol, molecular operating environment.

The rapid developments in our understanding of biomolecular structures and their direct relationship to function have transformed biochemistry to a new level. Integration of this knowledge in a readily available framework is critical and this can be achieved through visualization of three-dimensional structures of biomolecules using interactive computer graphics. In addition, molecular modeling plays an important role in structure-bas drug design in the pharmaceutical companies, biotechnology companies, and university research since it is useful in predicting structures of macromolecules, as well as for analyzing chemical and biological functions of these molecules. For these reasons, interactive molecular modeling has now become an integrated part of standard Biochemistry and/or Biomolecular Science courses taught at many universities. In this work, we present a relatively simple tutorial for a specific software package for such modeling exercises in a typical undergraduate classroom environment.

Currently, a number of molecular modeling software packages are used for teaching three-dimensional structures of biological macromolecules in undergraduate courses [1–15]. Many of these packages are available for free, and several tutorials illustrating simulation details as well as pedagogical aspects also are available. The present report is a result of our own efforts for several years in this area, and focuses on the software package, Molecular Operating Environment (MOE), developed by Chemical Computing Group Inc [16]. It should be noted at this time that neither our university nor we received any compensation for this work by this company. In earlier years, we have used Insight II as a visualization platform and developed tutorials for introductory biochemistry classes. Examples of macromolecules that were used in these tutorials include: hemoglobin, myoglobin, porins, membrane proteins, ferrodoxin-NADP+ reductase, and citrate-synthase. When our IBM RISC stations using the UNIX operating system came to the end of their lifetime we converted these tutorials to be used on PCs with MOE.

MOE is quite versatile and can be used on a wide variety of platforms ranging from Intel computers running Microsoft Windows™, Linux to Mac OS X, IBM eServer, Sun Microsystems, Hewlett-Packard, and SGI systems. This powerful program is generally available for classroom use at an academically discounted cost. We found the PC (Windows) platform most useful for our purposes, because essentially all of our computer labs and classrooms are equipped with PCs and students are more familiar with this mode of operation. In order to run MOE, at least 1 GB of free hard-disk space and at least 64 MB memory are required. Use of MOE for molecular modeling in these classes allows students to view, display, analyze, interpret and manipulate biomolecular data in a straightforward way by utilizing interactive three-dimensional computer graphics tools. The system integrates visualization, molecular modeling, protein modeling, cheminformatics and bioinformatics all in one program. Although there are other UNIX programs available we found this superior because the students spent less time

¶ To whom correspondence should be addressed. Tel.: 518-564-4119; Fax: 518-564-3169; E-mail: luckla@plattsburgh.edu.

TABLE I
Sample outline of the general course-structure

Topic	Hours
Course introduction	1
Search and gather information from the Internet, Protein Data Bank, Pub Med etc	2
Nuclear Receptor Superfamily	2
Why study ER	2
Molecular Operating Environment	2
Overview of the three dimensional structure of ER and EST	2
Observing the Hydrophobic pocket in the LBD	1
Conserved amino acids and their role	2
Observing hydrogen bond, ionic bond and cation-pi interactions in the protein	3
Surface properties of the protein	2
Structural and comparative studies of ER-LBD in complex with different ligands	4
In class oral presentations	4

learning the operating system and more time focused on the biochemistry aspects of the tutorials. MOE is versatile and flexible due to certain additional capabilities including the pharmacophore-based combinatorial library design, potential energy evaluations, docking, crystallographic system and electron density map visualization. By introducing the student to the initial suite of visualization programs they can easily move to more complex utilities of the system in later research projects or in their future careers.

This manuscript focuses on a specific application of MOE, where we describe the molecular structure of the ligand-binding domain of the human alpha-estrogen receptor (LBD-ER). A biochemical modeling project on the estrogen receptor (ER) is suitable for an introductory biochemistry class or an environmental class about endocrine disruptors in the environment. Students planning to use this tutorial should have some familiarity with basic protein chemistry as described in any standard Biochemistry textbook [17–20]. We have designed the tutorial with two objectives in mind: 1) to show the correlation between protein structure and function and to 2) introduce the students to the ligand binding properties of the ER. This tutorial will reinforce the concepts of hydrogen bonding and hydrophobic interactions that occur in ligand binding in steroid receptors. Most importantly students are introduced to computational biochemistry research. A brief outline of the general course-structure is presented in Table I.

METHODS

Working with the MOE Window

A typical MOE application window is shown in Fig. 1. The top tool bar contains all the basic commands that will be used in this tutorial and this is accessible by mouse click. The blank line below the top tool bar is used for command line computing that we will not use in this present tutorial. SEQ is used to open Sequence Editor Window and Cancel is used to cancel any job. A detailed description of the MOE Window can be accessed from the MOE Help menu. Here, we briefly summarize a number of main commands. The vertical tool bar on the far right is used for additional commands and is accessible again by mouse click. For example, under **System** one can open the Atom Manager Window. The *Builder* button will open the Molecule Builder

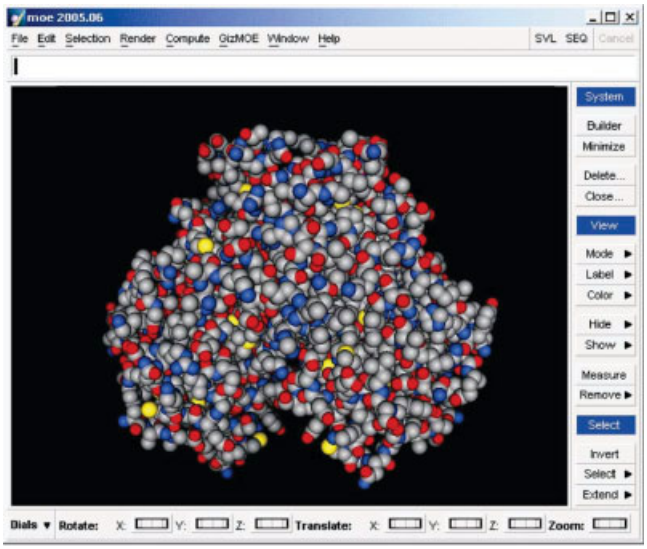

FIG. 1. **MOE Application Window**.

that allows one to construct small molecules or macromolecules or nucleotides. The *Minimize* button will perform Energy Minimization on the molecule in the window. The *Close* button can be used to clear molecular data. Using **View** it is possible to view the protein in different display *Modes* including line, stick, ball and line, ball and stick, and space filling. Among other standard MOE commands, *Label* is used to identify atom type, charge, or residue. *Color* is used to color specialized items such as specific atoms residues, chains, or secondary elements. *Hide and Show* are used to highlight or hide selected elements of structure. *Measure* is used to determine bond lengths, bond angles and dihedrals. The bottom part of the MOE window contains "dials" that are used for rotating, moving and zooming of molecule.

Data Input

To view the three-dimensional structure of LBD-ER complexed to 17β-estradiol (EST), a natural estrogen, the PDB file 1ERE.PDB [21] from the protein data base [22] was first edited to include data for only one dimer of the three found in the file. This edited file was then imported in the MOE window. Fig. 2A illustrates the structure of LBD-ER in ribbon form with EST displayed in space filling mode. The 2D structure of EST alone is shown in Fig. 2B.

RESULTS AND DISCUSSION

Why Explore the Structure of the ER?

Natural estrogens play a critical role in the normal growth, development and maintenance of a diverse range of tissues. They exert their effects via the ER which functions as a ligand activated transcription regulator. The ligand-binding domain of this protein is autonomous and has multiple functions including ligand binding, dimerization and ligand dependent transactivation [23]. Study of this part of the LBD-ER provides crucial information about the receptor function and steroid receptors in general.

X-ray crystal structures of the LBD-ER have been reported with a variety of ligands including EST, raloxifene, diethylstilbestrol, tamoxifen, genistein, and a num-

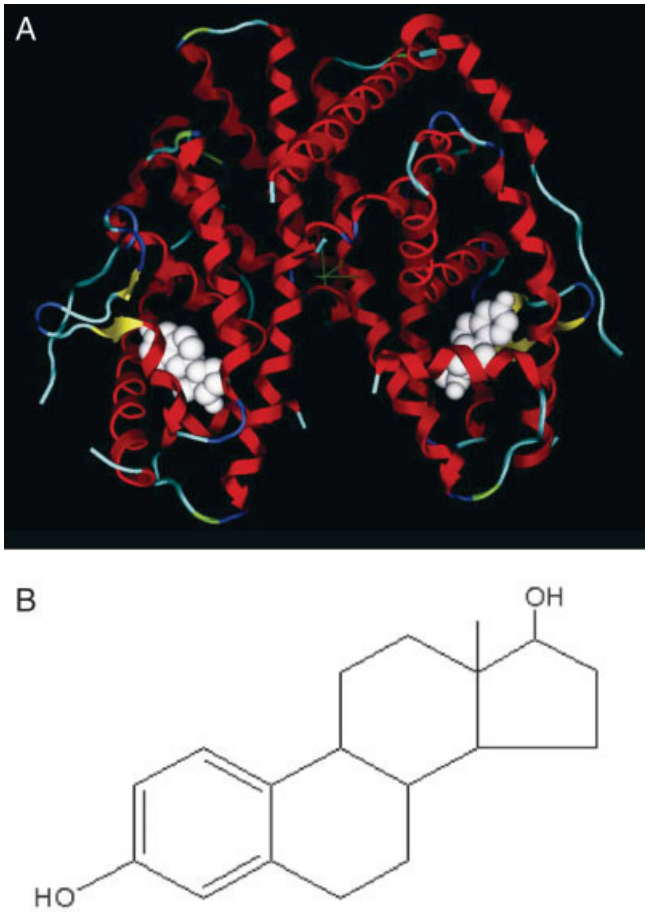

FIG. 2. (*A*) **Ribbon diagram of hERα LBD complexed with 17β-estradiol (white space filling mode)**. The figure shows the dimeric form of 1ERE.PDB. (*B*) Structure of 17β-estradiol ($C_{18}H_{24}O_2$).

ber of synthetic estrogens [21, 24–27]. LBD-ER binds a large repertoire of compounds with remarkable structural and chemical diversity. Most ligands have two hydroxyl groups separated by a rigid hydrophobic linker. They are classified as agonist or antagonist ligands by their effect on the structure and function of the protein. The three dimensional structure of LBD-ER as shown in Fig. 2*A* displays a canonical alpha-helical sandwich topology composed of 12 α helices that are arranged into three anti-parallel layers. This arrangement allows a sizeable buried binding pocket where the ligands are sequestered. In general, when an agonist binds in the pockets, helix 12 forms a "lid" over the binding pocket and exposes the transactivation site for coactivators. This binding is necessary for transcriptional activity. In contrast, when an antagonist binds to the pocket, it changes the conformation of the LBD such a way that helix-12 blocks the coactivator-binding site. Thus the orientation of helix 12 is an important factor for distinguishing agonist from antagonist. The underlying determination of the function of the LBD-ER with a particular ligand is revealed in its binding mode in the cavity. Exploration of the hydrogen bonding between ligand and protein and complementarity of the hydrophobic residues and the ligand give the students insight into steroid-ligand recognition. Further exploration of the protein architecture around EST reveals how the A ring pocket imposes a requirement for the planar ring group. The promiscuity of the LBD-ER is exhibited by the large unoccupied space above and below the steroid cavity.

Visualizing the Structure

Upon opening the MOE window and loading the data, use X, Y, and Z rotate wheels on the bottom of MOE window to rotate the molecule in the three planes. Zoom in by using the zoom tool located on the bottom of the screen. It is also possible to change the appearance of the protein (line/stick/ball and line/ball and stick or space filling) by using the Render menu from the top toolbar panel or Mode menu from the far right toolbar. Click on Render|Backbone|Color|Secondary Structure to view the Secondary structure of the protein or click on Render|Backbone|Color|Chain Color to color the Protein by Chain. To make viewing of the secondary structure easier, color the protein by clicking: Render|Backbone|Flat Ribbon. Viewing may be made even easier by hiding the backbone. To do this, click: Render|Hide|Backbone. Hide the sidechains by clicking on Render|Hide|Sidechain. Now we only can see the ribbons.

To view the EST in its binding site click: Render|Show|Ligand. To highlight it, open Sequence Editor. Highlight EST and, right click Atoms|Select and then Atoms|Show. EST will be displayed in the MOE window in pink. Change the appearance of the EST to space-filling mode by clicking Render| Space filling. In the MOE window, we can now see that the ligand-binding domain has the anti-parallel topology, with bound EST (Fig. 2*B*) in the lower portion of the domain (Fig. 2*A*).

View the dimer of 1ERE.PDB in stereo mode by clicking on Render|Stereo|left-Right. Adjust the stereoscopic view by zoom in or zoom out the molecule in the MOE window. View the protein by clicking on MOE|GizMOE|Rock and Roll. The protein in the MOE widow will then start to move slowly, and the three-dimensional structure of the molecule will become more apparent.

Save the molecular data by clicking: File|Save. You may want to save your molecular structural output either in moe format or in pdb format (e.g. *.moe). * is a wild card that represents any series of characters. You may also want to print the figure by clicking: File|Print (set the printer as postscript and select print to file option) and then save it as a postscript file (e.g., "ere.ps"). Or, you may save it on your computer using the Printer pull down menu. These choices are available depending on the printing devices installed on the computer. Details of saving and printing of a MOE file can be found on the help menu of MOE.

Observing the Hydrogen Bonding

To observe details of hydrogen bonding, click: Edit|Hydrogens|Add Hydrogen, then click: Render|Draw|Hydrogen Bonds. Before observing the hydrogen bonds,

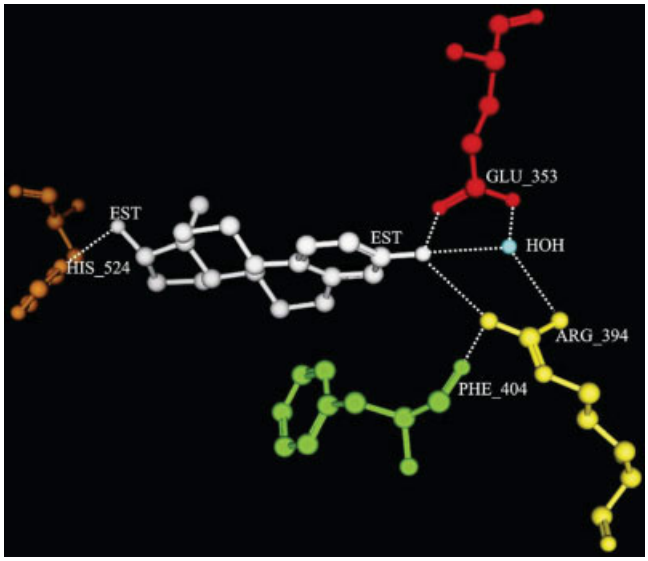

FIG. 3. **Hydrogen bonding between the 17β-estradiol (white) and the side chains of the ER protein in the ligand-binding pocket**. The side chains, His 524 (orange), Glu 353 (red), Phe 404 (green), and Arg 394 (yellow) are illustrated.

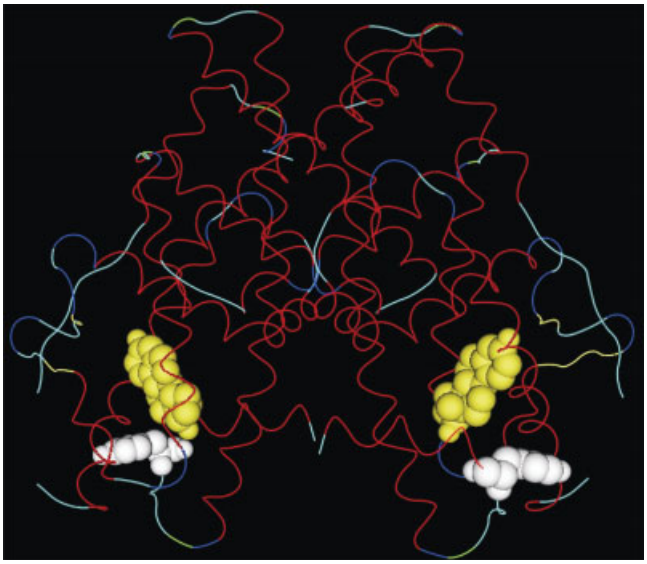

FIG. 4. **Alpha carbon backbone structure of 1ERE.PDB in dimeric form.** Tyr 537 (white) and 17β-estradiol (yellow) are shown in space filling mode.

display the backbone by clicking Render|Show|Backbone. Using MOE it is possible to display all or a selected set of hydrogen bonds in a given macromolecule. The contact analysis option of MOE (MOE|Compute|Biopolymer|Protein Contacts) reports hydrogen bond contacts within chains and/or between different chains. Both side-chain-to-side-chain and side-chain-to-main-chain hydrogen bond contacts can be calculated (see web-based supplementary material [28]). In Fig. 3, hydrogen bonding between 17β-OH of EST and δ nitrogen of His 524 is displayed. Here, Glu 353 in the ER accepts the H-bond donated by the 3-OH group of EST. The Arg 394 helps to keep the glutamate side chain in its right position via a structurally conserved H_2O mediated H bond. The side chain of Arg 394 is further supported by a H-bond to the carbonyl of a nearby Phe 404. A particular task for the students may be to trace the entire hydrogen-bonding network in the MOE window. They might also be asked to measure the hydrogen bond distances shown in Fig. 3.

Hydrophilic and Hydrophobic Regions

To display the hydrophilic residues of 1ERE.PDB in the MOE window, open Sequence Editor by clicking SEQ OR click on Window|Sequence Editor. In the sequence editor, click: Selection|Conserved Residues|Hydrophilic. This will highlight all the hydrophilic residues. To display these residues on the protein, click: Selection|Atoms|Of Selected Residues. The hydrophilic residues will now be displayed in pink on the protein. Repeat the same procedure to observe the hydrophobic residues of the protein. Be sure to select chains before selecting conserved residues. The contact analysis option of MOE can also be used to identify hydrophobic and ionic contacts (salt bridges), in this way, students can browse and isolate contacts in both the Sequence Editor and main MOE window [28].

Other Noncovalent Interactions

Cation-pi interactions play a crucial role in protein folding and stability [29, 30]. There are several papers that describe and demonstrate the importance of such interactions in the framework of undergraduate Biochemistry course [31, 32]. The CaPTURE program by Gallivan and Dougherty is an authoritative source for identifying energetically significant cation-pi interactions within proteins in the Protein Data Bank [33]. Although such interactions are often involved in ligand binding, the EST in 1ERE is not involved in such interactions. So it would be useful to leave this as an assignment for the students to determine whether there would be such an interaction between the protein and EST.

Another example of non-covalent interactions is the salt bridge, which also is important in protein stability and folding. The contact analysis option of MOE can identify ionic contacts (salt bridges) in the protein. The unique salt bridge that stabilizes the agonist conformation in 1ERE is between Arg-548 (end of helix 12) and Glu-523 (helix 11). Another relevant intra-molecular protein salt bridge is formed between Glu353 and Arg394 that are adjacent to the ligand binding pocket. A particular task for the students would be to identify each of them in the MOE window.

Amino Acids in the Binding Site

Particular amino acid sequences in the binding site are necessary for the receptor to bind ligands. MOE has a very versatile tool to display and identify particular amino acids. To display a specific amino acid of 1ERE.PDB in the MOE window, open Window|Sequence Editor. In the Sequence Editor window, click: Selection|Residue Selector. In the Residue Selector window, click on the amino acid of your choice; for example, Histidine—HIS or H. Then Click on Select Atoms and finally close the Residue

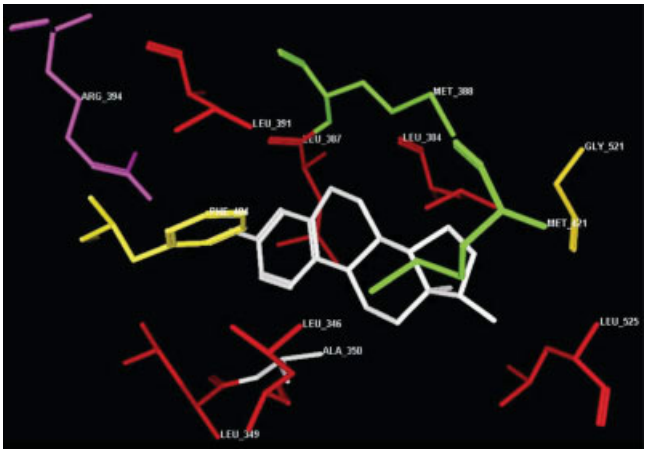

FIG. 5. **Critical residues in the binding pocket of the ER illustrated in stick form are depicted in this figure.** Illustrated are Ala 350 (white), Arg 394 (violet), Gly 521 (dark yellow), Leu 346, 349, 384, 387, 391, 525 (Red), Phe 404 (yellow), Met 388, 421 (green), and 17β-estradiol in white.

selector window. This will highlight all the Histidine residues of the pdb file in the MOE window. From the previous section, we know that the important amino acids in the binding pocket include Glu 353, Arg 394, and His 524. Students can easily locate these residues in the MOE application window. Koffman *et al.* reported that tyrosine has an important role in the binding of EST in ER [34]. According to Anstead *et al.* [35], Tyr 537 may have a controlling role in ligand binding because Tyr 537 lies at the start of helix 12. Tyrosine 537 is highlighted and shown in Fig. 4.

Students can be guided to observe some of the other critical residues in and near the active site. These are highlighted in Fig. 5. This include: Ala 350 (white) Arg 394 (violet), Gly 521 (dark yellow), Leu 346, Leu 349, Leu 387, Leu 384, Leu 391, Leu 525 (Red), Phe 404 (yellow), Met 388, Met 421(green). Another student task would be to locate Ile 424, Leu 354, Leu 428, Leu540, Met 343, Met 522, Met 528, Phe 425, Val 534 in order to determine each of the residue's orientation to the ligand and to each other.

Surface Representation

Using MOE, the students can create, display, and manipulate the molecular *surface* of a biomolecule. With this method, AnalyticConnolly, GaussAccessible, GaussConnolly, and Interaction surface of a biomolecule can be displayed [16]. To operate this mode in the MOE window one needs to click Compute|Molecular Surfaces. A dialogue box will appear. In the dialogue box for surface type, click: Interaction. Set the spacing at 0.75, and set the render as solid with transparency set to 0. This will generate the Interaction surface for the protein. To remove the radii by clicking Window|Graphic Objects, choose the surface and click Hide. Similar protocols are used to display the GaussConnolly surface of the biomolecule as shown in Fig. 6. The two later surface renderings reinforce the importance of these surface hydrophilic and hydrophobic interactions in the formation of the LBD

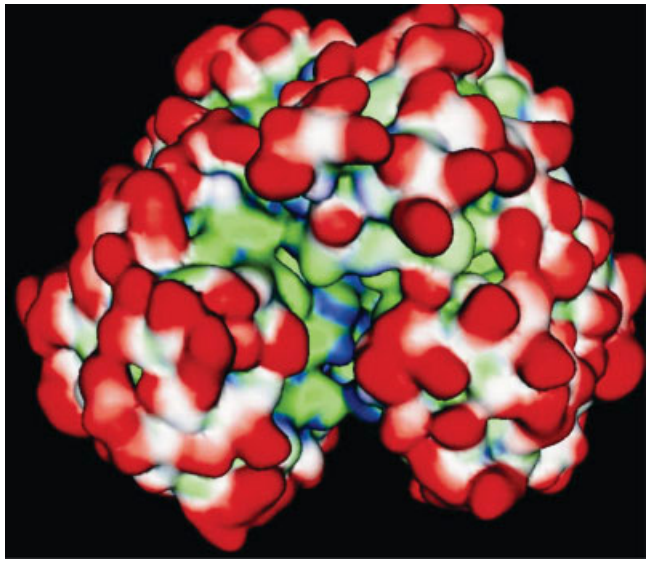

FIG. 6. **GaussConnolly surface of 1ERE.PDB.** This depiction represents pocket areas on the protein. The red areas represent nonpocket regions or peninsula regions, while the white areas represent neutral regions. The blue and green areas are hydrophilic and hydrophobic pockets, respectively.

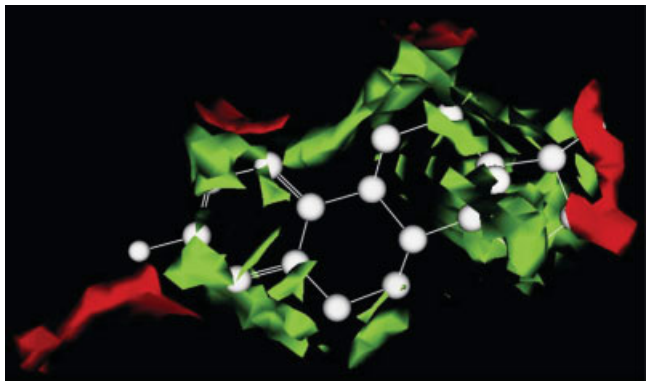

FIG. 7. **Contact Statistics plots of 1ERE.PDB.** EST is shown in the white ball and line mode. The green solid area is hydrophobic when the settings are at 90% and red is hydrophilic at 90%.

dimer. The contrast in color allows the students to identify the areas of the biomolecule that will be solvent accessible and available for hydrogen bonding. They will also be able to understand where the two lobes of the dimer interact and why this happens. Students can also visualize the hydrophilic areas of the surface away from the dimer interaction.

Contact Statistics

The structure of the LBD-ER shows a dimer that is stabilized by hydrophobic interactions. All nuclear receptors have a hydrophobic core in which a specific ligand binds.

To find out the receptor's contact preference in this process, open: Compute|Contact Statistics Grid. In the MOE window select EST atoms. Now in the contact Statistics window panel set the Atoms to be Unselected in any chain. Press the Apply button. We will see the con-

tact statistics plots of the ER's preferences along with the ligand (Fig. 7).

FUTURE TASKS

By using the tutorial presented here, it is possible to engage students in exploring the structure of ligand-binding domain (LBD) of the ER when complexed with diethylstilbestrol (3ERD.PDB), 4-hydroxytamoxifen (3ERT.PDB), and raloxifene (1ERR.PDB). It is also possible to assign the task of identifying, superposing and comparing the structures of beta ligand-binding domain complexed with full antagonist raloxifene (1QKN.PDB), and partial agonist genistein (1QKM.PDB).

REFERENCES

[1] R. A. Sayle, E. J. Milner-White (1995) Rasmol: Biomolecular graphics for all, *Trends Biochem. Sci*. **20**, 374–376.

[2] E. Martz (2002) Protein explorer: Easy yet powerful macromolecular visualization, *Trends Biochem. Sci*. **27**, 107–109.

[3] D. C. Richardson, J. S. Richardson (1992) The kinemage: A tool for scientific communication, *Protein Sci*. **1**, 3–9.

[4] S. W. Weiner, P. F. Cerpovicz, D. W. Dixon, D.B. Harden, D. S. Hobbs, D. L. Gosnell (2000) RasMol and Mage in the undergraduate biochemistry curriculum, *J. Chem. Educ*. **77**, 401–406.

[5] W. L. DeLano (2002) The PyMOL molecular graphics dystem, http://www.pymol.org.

[6] Jmol, www.jmol.org.

[7] Swiss-PdbViewer (DeepView). http://ca.expasy.org/spdbv/.

[8] S. Bottomley, D. Chandler, E. Morgan, E. Helmerhorst (2006) jAMVLE, a new integrated molecular visualization learning environment, *Biochem. Mol. Biol. Educ*. **34**, 343–349.

[9] L. Grell, C. Parkin, L. Slatest, P. A. Craig (2006) EZ-Viz, a tool for simplifying molecular viewing in PyMOL, *Biochem. Mol. Biol. Educ*. **34**, 402–407.

[10] R. C. Bateman, D. Booth, R. Sirochman, J. Richardson, D. Richardson (2002) Teaching and assessing three-dimensional molecular literacy in undergraduate biochemistry, *J. Chem. Educ*. **79**, 551–552.

[11] D. C. Richardson (2002) Teaching molecular 3-D literacy, *Biochem. Mol. Biol. Educ*. **30**, 21–26.

[12] D. W. Sears (2002) Using inquiry-based exercises and interactive visuals to teach protein structure/function relationships, *Biochem. Mol. Biol. Educ*. **30**, 208.

[13] G. R. Parslow (2002) Commentary: Molecular visualization tools are good teaching aids when used appropriately, *Biochem. Mol. Biol. Educ*. **30**, 128–129.

[14] R. R. Peterson, J. R. Cox (2001) Integrating computational chemistry into a project-oriented biochemistry laboratory experience: A new twist on the lysozyme experiment, *J. Chem. Educ*. **78**, 1551–1555.

[15] A. Herraez (2006) Biomolecules in the computer—Jmol to the rescue, *Biochem. Mol. Biol. Educ*. **34**, 255–261.

[16] MOE (The Molecular Operating Environment) Version 2005.06, software available from Chemical Computing Group Inc., 1010 Sherbrooke Street West, Suite 910, Montreal, Canada H3A2R7. http://www.chemcomp.com.

[17] D. Voet, J. G. Voet, C. W. Pratt (2002) *Fundamentals of Biochemistry*, Upgrade ed., Wiley, New York.

[18] R. H. Garrett, C. M. Grisham (1999) *Biochemistry*, 2nd ed., Saunders College Publishing, New York.

[19] D. L. Nelson, M. M. Cox (2005) *Lehninger Principles of Biochemistry*, 4th ed., W. H. Freeman, New York.

[20] J. M. Berg, J. L. Tymoczko, L. Stryer (2006) *Biochemistry*, 6th ed., W.H. Freeman, New York

[21] A. M. Brzozowski, A. C. Pike, Z. Dauter, R. E. Hubbard, T. Bonn, O. Engstrom, L. Ohman, G. L. Greene, J. A. Gustafsson, M. Carlquist (1997) Molecular basis of agonism and antagonism in the oestrogen receptor, *Nature* **389**, 753–758.

[22] Protein Data Bank, www.rcsb.org/pdb.

[23] M. J. Tsai, B. W. O'Malley (1994) Molecular mechanisms of action of steroid/thyroid receptor superfamily members, *Annu. Rev. Biochem*. **63**, 451–486.

[24] A. K. Shiau, D. Barstad, P. M. Loria, L. Cheng, P. J. Kushner, D. A. Agard, G. L. Greene (1998) The structural basis of estrogen receptor/coactivator recognition and the antagonism of this interaction by tamoxifen, *Cell* **95**, 927–937.

[25] A. C. W. Pike, A. M. Brzozowski, R. E. Hubbard, T. Bonn, A. Thorsell, O. Engstrom, J. Ljunggren, J. Gustafsson, M. Carlquist (1999) Structure of the ligand-binding domain of oestrogen receptor beta in the presence of a partial agonist and a full antagonist, *EMBO J*. **18**, 4608–4618.

[26] A. C. W. Pike, A. M. Brzozowski, R. E. Hubbard (2000) A structural biologist's view of the oestrogen receptor, *J. Steroid Biochem. Mol. Biol*. **74**, 261–268.

[27] D. M. Tanenbaum, Y. Wang, S. P. Williams, P. B. Sigler (1998) Crystallographic comparison of the estrogen and progesterone receptor's ligand binding domains, *Proc. Natl. Acad. Sci. USA* **95**, 5998–6003.

[28] http://people.clarkson.edu/∼urmi/ER/index.htm.

[29] J. P. Gallivan, D. A. Dougherty (1999) Cation-pi interactions in structural biology, *Proc. Natl. Acad. Sci. USA* **96**, 9459–9464.

[30] C. Ma, D. A. Dougherty (1997) The cation-pi interaction, *Chem. Rev*. **97**, 1303–1324.

[31] J. R. Cox (2000) Teaching noncovalent interactions in the biochemistry curriculum through molecular visualization: The search for π interactions, *J. Chem. Educ*. **77**, 1424–1428.

[32] D. W. Honey, J. R. Cox (2003) Lesson plan for protein exploration in a large biochemistry class, *Biochem. Mol. Biol. Educ*. **31**, 356–362.

[33] CaPTURE program, http://capture.caltech.edu/.

[34] B. Koffman, K. J. Modarress, T. Beckerman, N. Bashirelahi (1991) Evidence for involvement of tyrosine in estradiol binding by rat uterus estrogen receptor, *J. Steroid Biochem. Mol. Biol*. **38**, 135–139.

[35] G. M. Anstead, K. E. Carlson, J. A. Katzenellenbogen (1997) The estradiol pharmacophore: Ligand structure-estrogen receptor binding affinity relationships and a model for the receptor binding site, *Steroids* **62**, 268–303.

Genetically Engineered Protein Films on the Quartz Crystal Microbalances: A Biosensor for the Detection of Xenoestrogens

Linda A. Luck, Adam Layhee, David Abramowitz, Laurel J. Standley, Ruthann A. Rudel

Department of Chemistry, State University of New York, Plattsburgh, NY USA 12901

Substantial evidence indicates that endocrine disrupting chemicals (EDCs) particularly those that interact with the estrogen receptor may play a role in endocrine related cancers particularly breast cancer. EDCs are found in food, water, air and consumer products and originate from pharmaceutical, industrial, agricultural and natural sources. Using current available technologies it is extremely difficult to identify EDCs in complex sample mixtures. Hence we have developed a new technology, an estrogen-receptor quartz crystal microbalance biosensor (ER-QCM) for the selective detection of estrogenic substances. The ER-QCM using genetically engineered proteins immobilized on the gold surface of the piezoelectric crystal has been shown to detect estradiol, tamoxifen and genistein which are know ligands of the estrogen receptor. In addition the biosensor shows no response for non-binding ligands such as testosterone.

The ER-QCM sensor surface is the unique and critical aspect of this biosensor that permits the detection of ligands which bind to the estrogen receptor. Immobilization of the hormone binding domain of the estrogen receptor (HBD) to the surface is accomplished by Au-S bond from a sulfur atom in a cysteine residue on the protein to the gold on the crystal surface. HBD has four native cysteine residues (530, 447, 417, and 381). Cysteine 447 is buried while the other three are surface exposed. Our initial studies used a construct of the ER-HBD where residues 530 and 381 were changed to serines and 417 remained the only surface exposed cysteine. This allows a uniform orientation of protein on the surface.

In this study we will show a new repertoire of ligands that are sensed by the ER-QCM with cysteine 417 immobilization. In addition, we have recently prepared another mutant where 381 and 417 are mutated to serine residues and 530 remains as a cysteine residue. This new mutant of HBD is oriented on the surface in a manner quite different than the protein from our previous studies since the 530 residue is near the binding pocket. Comparison of the two mutants and their binding abilities with the various ligands will be presented. A third mutant with all three surface exposed cysteines mutated to serines was generated as a control and proof that the cysteine residues are necessary for creating a self assembled protein layer on the surface of the crystal.

We gratefully acknowledge funding for this work from NSF grant CTS-0329698 and US Army Breast Cancer Research Grant Concept Award W81XWH-06-1-0621.

Genetically Engineered Protein Films on Gold Nanoparticles: A Novel Electrochemical Glucose Biosensor

Linda A. Luck[1] and Silvanna Andreescu[2]
[1]Department of Chemistry, Plattsburgh State University, Plattsburgh, NY USA 12901
[2] Department of Chemistry, Clarkson University, Potsdam, NY USA 13699

The construction of an electrochemical biosensor for the selective detection of glucose using gold nanoparticles has been investigated. We have studied the surface chemistry and the interactions of gold nanoparticles with a native and genetically engineered *E.coli* periplasmic protein that binds glucose and galactose (GGR). The recent popularity and utilization of periplasmic binding proteins as the sensing units of biosensors has arisen due to their solubility, stability and ability to reversibly bind a large variety of small ligands including sugars, amino acids and inorganic ions. These proteins comprise a large family of functionally similar receptors with a two-domain structure and a hinge cleft mechanism for binding substrates. The wild-type GGR does not have native cysteine residues. The genetically engineered GGR with cysteine at the N-terminus (GGRA1C) can form directed, self-assembled protein films on gold surfaces via a covalent bond with the sulfur. UV, Zeta potential, Particle Size Distribution and TEM analysis was performed on the gold nanoparticles that were incubated with GGR and GGRA1C. The gold colloid particles with GGRA1C showed distinctively different characteristics than those exposed to GGR. The genetically engineered amino acid cysteine residue is key to the immobilization strategy for this biosensor.

Cyclic voltammetry was used to detect the binding of glucose to GGRA1C-modified nanoparticles. Non-binding substrates do not elicit a change in response. We show that this electrochemical biosensor is suitable for selective determination of glucose with a detection limit of 0.25 micromolar. Our biosensor offers several advantages over current technologies, including simplicity, selectivity and sensitivity. The results indicate that this technique will find widespread use for variety of protein receptors including those of the steroid superfamily.

We gratefully acknowledge funding for this work from NSF grant CTS-0329698 and US Army Breast Cancer Research Grant Concept Award W81XWH-06-1-0621.

Detection of Small Ligands using a Quartz Crystal Microbalance with Genetically Engineered Protein Receptors

Ruth E Baltus
Department of Chemical and Biomolecular Engineering
Clarkson University
Potsdam, NY 13699-5705

Linda A. Luck
Department of Chemistry
SUNY Plattsburgh
Plattsburgh, NY 12901

Kendra S. Carmon
Department of Integrative Biology and Pharmacology
UT Houston Health Science Center
Houston, TX 77030

We will present results from experimental investigations of quartz crystal microbalance (QCM) biosensors that utilize genetically engineering protein receptors. The *E. coli* periplasmic glucose/galactose binding protein (GGR) and the hormone-binding domain of the human estrogen receptor α (HBD) were utilized as biological recognition elements in these studies. The sugars glucose and galactose bind to GGR; natural estrogens and xenoestrogens bind to HBD. Mutant proteins of HBD and GGR were genetically altered to create a single, solvent exposed cysteine in order to immobilize the proteins on the gold surface in self assembled protein monolayers (SAPM). It has been shown that all mutant proteins bind to respective ligands with near native affinities.

In this study, the frequency shift resulting from protein attachment to the gold electrode as well as the frequency response resulting from subsequent exposure of the SAPM to ligand was measured. The frequency response to protein immobilization for both proteins was in general agreement with the Sauerbrey prediction for addition of a rigid mass to the surface. These calculations relied on estimates of protein size provided by crystallography. The frequency response resulting from ligand binding was observed to be considerably larger than predicted from the Sauerbrey equation.

We hypothesize that the frequency shift observed when the SAPM is exposed to ligand arises from the QCM sensing conformational changes of the proteins that occur with ligand binding. Further studies show that the QCM can only sense these ligand induced conformational changes when the proteins are directly bound to the surface via the sulfur-gold bond. These observations are important in that they illustrate a widened applicability of QCM to protein systems that bind small molecules and undergo ligand-induced conformational changes.

Biosensors Using Genetically Engineered Proteins: Incorporating Undergraduates in Interdisciplinary Research Projects in the Biosensor Field

Clarkson University, a primarily undergraduate institution, provides a broad range of opportunities for students in basic science and engineering biosensor research under the mentorship of an interdisciplinary group of scientists and engineers. The students are exposed to the research process from design to analysis to authorship, with the goals of instilling both an understanding of the research process and of fostering a commitment to the pursuit of their part of an interdisciplinary biosensor research project.

The students are recruited early in their education and participate for credit as an independent study course or for Honors/Senior thesis work. The capstone experience involves a presentation of the work in a public forum either as a poster or powerpoint presentation to their peers and faculty.

Receptor proteins can be used as the sensing element in biosensors for measuring small compounds. One of the major challenges in the development of biosensors has been in immobilizing receptors on surfaces while controlling their orientation so that full biological activity is maintained. It has been shown that the receptors from *E.coli* can be been genetically reconstructed and used as the platform in biosensors where ligand-induced structural changes in the protein allow detection of an analyte. To this end, my laboratory students have utilized genetic engineering to incorporate a cysteine residue into a number of periplasmic receptors and human steroid receptors. This allows for the *direct* immobilization of the protein to a gold surface via a sulfur-gold covalent linkage. The individual self-assembled monolayers of were capable of specifically binding target ligands, as revealed by surface plasma resonance, electrical impedance spectroscopy, cyclic voltametry, atomic force microscopy, and by the response in an electrochemical quartz crystal microbalance.